Reviewed Preprint
v1 • October 13, 2025
Not revised

Reviewed Preprint
v2 • June 25, 2026
Revised by authors

For correspondence:
mario.svirksy@med.nyu.edu
robert.froemke@med.nyu.edu

Competing interests: No competing interests declared

Funding: See page 27

Reviewing editor: Brice Bathellier, Centre National de la Recherche Scientifique, France

Distinct cortical encoding of acoustic and electrical cochlear stimulation

Ariel Edward Hight[1,2,3], Michele N Insanally[2,3,4,5], Julia K Scarpa[2,3], Yuko Tamaoki[1,2,3], Rohit Makol[1,2,3,6], Yew-Song Cheng[2], Michael Trumpis[7], Jonathan Viventi[7,8,9,10], Mario A Svirsky[1,2,3] ✉, Robert C Froemke[1,2,3] ✉

[1]Translational Neuroscience Institute, New York University Grossman School of Medicine, New York, United States • [2]Department of Otolaryngology-Head and Neck Surgery, New York University Grossman School of Medicine, New York, United States • [3]Department of Neuroscience, New York University Grossman School of Medicine, New York, United States • [4]Department of Otolaryngology, University of Pittsburgh School of Medicine, Pittsburgh, United States • [5]Department of Neurobiology, University of Pittsburgh School of Medicine, Pittsburgh, United States • [6]University of Connecticut School of Medicine, Storrs, United States • [7]Department of Biomedical Engineering, Duke University, Durham, United States • [8]Department of Neurobiology, Duke University School of Medicine, Durham, United States • [9]Department of Neurosurgery, Duke University School of Medicine, Durham, United States • [10]Department of Neurology, Duke University School of Medicine, Durham, United States

eLife Assessment

This **valuable** study compares auditory cortex responses to sounds and cochlear implant stimulation measured with surface electrode grids in rats. Beyond the reduced frequency resolution of cochlear implants observed previously, this study suggests key discrepancies between neuronal representations of cochlear stimulations and natural sounds. The evidence for this result is **solid** but could be strengthened with a clarification of the methodology and an adaptation of the claim to the actual precision of the measurements. This study is of interest to researchers in the auditory neuroscience field and clinicians implementing treatments with cochlear implants.

https://doi.org/10.7554/eLife.108550.2.sa4

Abstract

Cochlear implants are neuroprosthetic devices that restore hearing and speech comprehension to profoundly deaf humans, and represent an exemplar application of biomedical engineering and research to clinical conditions. However, the utility of these devices in many subjects is limited, largely due to lack of information about how neural circuits respond to implant stimulation. Recently we showed that deafened rats can use cochlear implants to recognize sounds, and that this training refined the responses of single neurons in the primary auditory cortex. Here we asked how local populations of cortical neurons represent acute implant stimuli, using electrode arrays we developed for cortical surface recordings for micro-electrocorticography (μECoG), a form of intracranial electroencephalography (iEEG). We found that there was a limited tonotopic organization across recording sites, relative to a clearer tonotopic spatial representation in normal-hearing rats. Singletrial iEEG responses to acoustic inputs were more reliable than responses to cochlear implant stimulation, although stimulus identity could be successfully decoded in both cases. However, the spatiotemporal response profiles to acoustic vs cochlear implant stimulation were substantially different. Decoders trained on acoustic responses showed essentially zero information transfer when tested on electrical stimulation responses in the same animals after deafening and cochlear implant stimulation. Thus while acute cochlear implant stimulation might activate the auditory cortex in a cochleotopic manner, the dynamics of network activity are quite distinct, suggesting that pitch percepts from acoustic and electrical stimulation are fundamentally different.

Introduction

Cochlear implants are neuroprosthetic devices that restore hearing and provides users with an ability to attain open-set speech perception without other aids such as lip-reading (Djourno and Eyries, 1957; Simmons et al., 1965; Michelson, 1971; House and Urban, 1973; Eddington et al., 1978; Hochmair and Hochmair-Desoyer, 1981; Wilson et al., 1991; Clark, 2006; Svirsky, 2017). Cochlear implants function by inserting a single and flexible shank of electrodes along the cochlear spiral (generally 12-22 channels in human subjects), to stimulate primary afferent neurons of the auditory system and bypass pathologies of deafness. Individual electrodes deliver trains of electrical pulses, providing spectral cues as a function of location along the topographical axis of the cochlear spiral, mimicking the encoding of sound in a functional and healthy cochlea. Over 1 million users have been implanted world-wide, making it the most widely adopted type of brain-computer interface, surpassing vagus nerve stimulators, deep-brain stimulation electrodes, and artificial retinas (Hays et al., 2013; Dawson et al., 2016; Ayton et al., 2020; Zeng, 2022; Johnson et al., 2024). Cochlear implants are thus the gold-standard for neuroprosthetic device use in terms of performance, safety, and ability to fine-tune or personalize the programming of each device to individual users.

Despite their wide adoption in human subjects over the last several decades, there is limited understanding of how these devices restore functionality and the sense of hearing to users. One long-standing question has been how the central auditory system responds to and interprets signals resulting from electrical stimulation of auditory nerve fibers. It is unknown to what degree emulating the patterns evoked by acoustic stimulation in normal hearing users is important for the auditory system to interpret patterns of evoked neural activity and inform downstream auditory perception. Many structures of the central auditory system are organized tonotopically, following the frequency alignment of the cochlear basilar membrane (Walzl and Woolsey, 1946; Merzenich et al., 1973; Polley et al., 2007). This topographic mapping might facilitate the encoding of auditory stimuli. While previous studies have demonstrated cochleotopic organization in auditory cortex of cochlear implant animals (Bierer and Middlebrooks, 2002; Johnson et al., 2016), a fundamental question remains unanswered: does electrical stimulation of specific cochlear locations elicit the same cortical representations and perceptual qualities as acoustic stimulation of corresponding frequencies? The spatiotemporal dynamics of these representations and how they relate to acoustic processing in normal hearing individuals remain unclear. Previous psychophysical studies in human implant users have provided indirect evidence for perceptual differences (McDermott, 2004) and similarities (Vermeire et al., 2013), but direct neural evidence comparing representations in the same subjects has been lacking. This question has profound implications for how we design and program cochlear implants, or more generally other brain-computer interface devices.

Studies in non-human animals are required to understand the neural basis of cochlear implant use and the relation to spatiotemporal representations in the auditory system. Responses to cochlear implant stimulation have been studied in a number of species generally in non-behaving animals under anesthesia (Klinke et al., 1999; Bierer and Middlebrooks, 2002; Middlebrooks and Bierer, 2002; Fallon et al., 2014; Johnson et al., 2016, Adenis et al. 2024), but occasionally in awake or behaving animals (Vollmer and Beitel, 2011; Keating et al., 2013; Johnson et al., 2016). Over the last decade we have examined cochlear implant responses in deafened rats (King et al., 2016; Glennon et al., 2019), where we showed that animals can be trained to report the activation of specific implant channels. Behavioral training with the cochlear implant led to substantial plasticity within the deafened rat auditory cortex, modifying synaptic receptive fields and adjusting excitatory-inhibitory balance at the level of single neurons. Prior to training, the responses of single cells to implant stimulation were erratic and inhibition was mismatched relative to excitation. After training, inhibition became aligned with excitation across the array of implant electrode channels (Glennon et al., 2023). However, intracellular recording in vivo is infeasible in human subjects. Thus other approaches more amenable to clinical use are required, to measure neural coding of cochlear implant signals and enable translation of results from non-human studies to improve implant performance by human subjects.

Here we aimed to determine the spatiotemporal representations of implant channels beyond the responses of single neurons, but instead across a broader extent of rat auditory cortex. We take advantage of improvements in micro-electrocorticography (μECoG), a sub-type of intracranial electroencephalography (iEEG) that generally uses grid electrodes placed epi– or sub-durally over the cortical surface to measure local electrical activity (Insanally et al., 2016; Woods et al. 2018). iEEG recordings have high temporal precision, greatly improved signal-noise ratios, and better spatial resolution than conventional scalp EEG recordings (Abdi-Sargezeh et al., 2023; Janiukstyte et al., 2023). Signals reflect local electrical fields generated by aggregate neural activity in the regions adjacent to recording sites (Jasper and Penfield, 1949; Chang, 2015; Fukushima et al., 2015). iEEG has been used for studies of human brain organization particularly of speech and language centers, but these recordings are necessarily done in epileptic subjects to help locate seizure foci before surgical resection (Nourski et al., 2013; Mesgarani et al., 2014; Tang et al., 2017; Beynon et al., 2021; Norman-Haignere et al., 2022). Non-human animal studies remain essential for determining how sensory inputs are represented and processed in subjects without overt neurological conditions. To this end, we have designed and manufactured a novel and flexible 60-channel cortical surface iEEG array for adult rats, and validated that we can measure auditory responses and cortical map topography in normal hearing animals with these arrays (Insanally et al., 2016; Trumpis et al., 2017; Woods et al. 2018). Using these custom-fabricated iEEG grid electrodes, we now ask how auditory cortex responds to implant stimulation in untrained or trained deafened adult rats, and how different evoked signals and/or mesoscale tonotopic organization is in cochlear implant users vs normal-hearing animals.

Materials and Methods

Surgical procedure for iEEG recordings

All animal procedures were performed in accordance with National Institutes of Health standards and were conducted under a protocol approved by the NYU Grossman School of Medicine Institutional Animal Care and Use Committee. We used a custom array consisting of 61 passive electrodes spaced 406 μm apart in an 8 x 8 grid, with three corner electrodes omitted and the fourth corner electrode intentionally unexposed to test encapsulation, reducing the number of active recorded sites to 60 (Insanally et al., 2016). iEEG grids were fabricated using a standard flex-PCB processing technique by Microconnex Flex Circuits (Snoqualmie, WA). All procedures and experiments were carried out in a sound-attenuation chamber and under anesthesia.

A specific surgical protocol was developed for implantation of cortical surface iEEG in rats. Sprague-Dawley rats 4–6 months old were anesthetized with ketamine (40 mg kg−1, intramuscular injection) and dexmedetomidine (0.125 mg kg−1, intramuscular injection), or pentobarbital (50 mg kg−1, intraperitoneal injection). The head was secured in a custom head-holder that left the ears

unobstructed. A longitudinal incision was made along the midline to expose the skull. Five bone screws were inserted into the skull around the point of entry of the electrode array to help anchor the dental cement (C & B Metabond Quick! Luting Cement). After reflecting the right temporalis muscle, a 5 mm × 5 mm craniotomy was made on the right temporal skull to expose the brain, and a sterilized iEEG array was epidurally placed over the left hemisphere core auditory cortex, located using vasculature landmarks. A thin silver wire was soldered between the headstage and the skull screws to be used as ground and reference.

Surgical procedure unilateral cochlear implantation of the right ear

Cochlear implantation procedures are similar to our past studies (King et al., 2016; Glennon et al., 2023). 8-channel animal cochlear implant arrays (HL08) were provided by Cochlear Americas. The array contained platinum-iridium band electrodes coated in silastic and connected to a nine-pin Nanonics connector (TE Connectivity, Berwyn, PA) with a single, additional extracochlear ball ground. The ipsilateral pinna was pulled forward and secured with a hemostat, the head rotated laterally, and the post-auricular junction between the ear canal and the sternocleidomastoid muscle (SCM) is identified as the initial incision site. An incision was made and the superficial fascia of the neck was dissected to identify the facial nerve i.e., cranial nerve (CN) VII. Minor bleeding was controlled using hemostatic epinephrine-soaked cotton pellets (Epidri pellets; Pascal International, Bellevue, WA), applied with light pressure. The SCM and posterior belly of the digastric muscle (PBD) were dissected from the tympanic bulla (TB) ventral and rostral to the trunk of CN VII. The TB was cleared of muscle and periosteum; the periosteum of the bulla was kept in normal saline and used later to seal the cochleostomy site. The drilling of the TB was begun ventrorostral to the trunk of CN VII with a 0.5 mm diamond burr and continued dorsally with care taken to avoid injuring CN VII, until the SA overlying the RW was fully visualized. Any remaining tissue or debris was removed with microforceps before the cochleostomy was performed.

Prior to performing the cochleostomy and inserting the array, the array lead and connector were secured. The post-auricular incision was expanded dorsally toward the skull. An area 4-5 mm in diameter was cleared and cleaned to expose the occipital skull, and the connector was attached perpendicular to the skull using C&B-Metabond (Parkell, Edgewood, NY) and bone screws. The lead to the electrode array was then sutured to the trapezius muscle, allowing enough lead to remain free to facilitate motion required for array insertion. The lead to the separate ground electrode was similarly secured into small muscle pockets in the trapezius. The cochleostomy site was identified ~0.5 mm directly below the lip of the RW in the basal turn of the cochlea, identified by both the stapedial artery and the cochlear promontory in the tympanic space. The site was gently drilled with a 0.1 mm diamond burr, and the array was inserted into the scala tympani without resistance using AOS forceps (Cochlear, Sydney, Australia) until all of the platinum-iridium contacts were within the scala tympani. We required that all eight electrodes pass through the cochleostomy, confirming that the array was inserted in the direction of the apex. The array occludes most, if not all, of the drill site, but to minimize postsurgical perilymphatic leak strips of periosteum taken from the bulla were placed around the implant to seal the site, followed by application of high-grade cyanoacrylate (Surgi-lock 2oc; Meridian Animal Health, Omaha, NE). The remaining lead was cemented into the bulla with C&B-Metabond (Parkell). Before closure, a small square of gelfoam with dexamethasone was left on the root of the facial nerve to prevent inflammation and heal any minor damage that may have occurred.

Bilateral sensorineural hearing loss

The deafening procedure (mechanical only, as described and validated in Glennon et al. 2023) was identical to the cochlear implantation procedure, with the exception of the array being removed before closure. Following both array and gelfoam removal, the cochleostomy site was

closed with a trapezius muscle or periosteum graft, followed by 2-octyl cyanoacrylate (i.e., the array is removed from the cochlea). Both ears were deafened in this manner, but a functional array remained in the right ear for acute electrical stimulation.

Behavioral training for tone and implant channel detection

Four animals with iEEG recording electrodes were behaviorally trained to detect target tones. Rats were food restricted and trained on a self-initiated, auditory go/no-go task (Froemke et al., 2013; Martins and Froemke, 2015; King et al., 2016). Animals nosepoked in a designated port to initiate trials and are trained to nosepoke in a different port if the target tone was presented (22.6 kHz, any intensity) or withhold from nosepoking if a nontarget (foil) tone was presented (0.5-32 kHz excluding 4 kHz if 4 kHz was the target, or 8-45.3 kHz excluding 22.6 kHz if 22.6 kHz was the target, at 0.5-1 octave intervals and at any intensity). A sugar pellet reward was given for correct nosepokes within 2.5 s of target-tone presentation, whereas a 7 s timeout was given if the animal incorrectly nosepoked for foil tones. The four rats that achieved >70% target-tone hit rate and d' ≥1.7 were included for further testing and implantation. A second subset of three animals was behaviorally trained to detect cochlear implant channel 3 (n=2) or channel 4 (n=1); procedures were the same for tones except that a programmable clinical cochlear implant processor was used. These animals were trained for 3, 9, and 13 days.

Stimulus presentation for cortical sensory mapping in normal hearing rats

Tone presentation was similar to our previous study of iEEG responses in normal-hearing rats (Insanally et al., 2016). Pure tones 50 ms in duration with 2 ms cosine-squared ramps ranging from 0.5-32 kHz (0.5 octave spacing) were generated using an auditory processor (TDT System III RZ6) and presented at a pseudorandom sequence at a rate of 1.25 Hz to the contralateral (right) ear using a calibrated free-field speaker (MF1 Multi-Field Magnetic Speaker, Tucker-Davis Technologies). Each tone was repeated 30 times at 70 dB SPL. The calibrated speaker exhibited <1% harmonic distortion and a flat output in the frequency range used.

Stimulus presentation for cortical sensory mapping in cochlear implanted rats

Electrical stimulation was delivered by an off-the-shelf Nucleus Freedom system speech processor (Cochlear) in which its transmitter coil drove a CI24RE implant emulator, where its output was connected to the implanted electrodes. The implant emulator is a standard clinical cochlear implant that is mounted in a plastic box with a DB-25 connector (Cochlear). We created a pigtail wire with a DB-25 connector and an Omnetics/Nanonics connector (Omnetics/TE Connectivity) to couple the emulator to the skull-anchored connector. The skull-anchored connector is also an Omnetics/Nanonics connector that is directly attached to the implanted array. All stimuli were based off standard parameters for cochlear devices including charge-balanced biphasic pulses with 8 μs interphase gaps and 25 μs/phase (total pulse width = 58 μs), presented at 900 pulses per second and configured in monopolar configuration where currents were driven between a single intracochlear electrode and the external ground electrode. For about half of tested animals (N=3), auditory stimulation activated the implant through the microphone of the speech processor via tones presented to each individual electrode's frequency allocation. The remaining cochlear implanted animals (N=4) were stimulated directly; the CI24RE implant emulator was driven by a Freedom system speech processor connected through the Freedom Programming Pod to a personal computer running the Custom Sound EP software (Cochlear). The Custom Sound EABR function was used (5 stimulation pulses presented at 900 pulses per second) to program and deliver stimuli to the implant.

Cochlear implant programming

Impedance and threshold measurements were obtained intraoperatively using Custom Sound EP (Cochlear) and were used for the initial programming of the sound processor. Electrically-evoked compound action potential (ECAP) thresholds were obtained and used to set the maximum stimulation level and the minimum stimulation level was set to 30 'clinical units' below the maximum level, equivalent to 4.7 dB in the CI24RE implant emulator (Azadpour and McKay, 2012). All additional settings typically deployed in a clinical setting, such as ADRO, were turned off (Custom Sound, clinical programming software for Nucleus Freedom).

ECAP measurements

Rats acutely implanted with an 8-channel cochlear implant were measured for ECAPs by stimulating and recording from the array of implanted electrodes, with an additional reference electrode implanted subdermally in the neck, using a cochlear implant emulator and a custom software program written in MATLAB and Python and using the Nucleus Implant Communicator (NIC, Cochlear Ltd.). All ECAP measures used the "ABCD" artifact removal technique (Brown et al. 1990) with a probe-masker interval of 0.5 ms, and a similar artifact removal for forward masking measures that was modified from the ABCD technique to compensate for different masker electrode configurations (Azadpour et al. 2021). The sense/recording electrode was selected as two channels apical to the probe; if that channel was not available, then the sense was selected as two channels basalward. In cases where the masking electrode was the same as the sense electrode, the sense was switched to the electrode closer to the probe, and the corresponding masked ECAP was scaled relative amplitudes of the probe-evoked masker-free ECAP measured at the two different sense electrodes. After impedance measurements were made to confirm the device was correctly implanted, configured, and within safe/compliant limits, ECAP thresholds were estimated for each electrode by manually stepping up and down stimulation levels specific to the manufacturer's programming units by steps of 5, until evoked ECAP amplitudes were of ~100 μV. Next, a forward masking paradigm was implemented to measure channel interaction and temporal recovery. For channel interaction, probe electrodes were preceded by a masker electrode by 0.5 ms, and masker electrode was roved from channel 1-8 to extract spatial tuning functions for each probe electrode. For temporal recovery, a masker stimulus was delivered on the electrode as the probe and the masker-probe interval was roved to capture temporal tuning functions for each probe electrode.

Processing of cortical iEEG recordings

All signal processing and analyses were performed using custom MATLAB scripts (MathWorks, MA). To determine whether trials were functional or contained artifacts, raw measurements were first filtered (2-150 Hz, 6^{th} order bandpass IIR filter) and then root mean squared power (rms) was computed for each channel. All trials with rms 20-300 μV were considered functional; power less than 20 μV corresponded with pre-amplifier saturation, while power greater than 300 μV consistently indicated intermittent corruption from non-neural sources. To then process functional recordings, we first used a notch filter to remove 60 Hz noise and 90, 120, 180 Hz harmonics. Recorded signals were then downsampled from 20 to 2 kHz using the decimate function (MATLAB), performing also the function of low-pass (anti-alias) filter and thereby rejecting any artifacts resulting from electrical stimulation delivered by cochlear implant electrodes.

Event-related potentials (ERPs) were extracted from raw downsampled recordings by further bandpass filtering (2-100 Hz) using a digital zero-order 6^{th} order Butterworth filter. Magnitudes of evoked ERP transients were measured by first rectifying measurements using the MATLAB abs() function and then subtracting the maximum of the baseline amplitude in the 50 ms pre-stimulus period (averaged over ±1 timestep) from the maximum of evoked amplitude in the 50 ms post-stimulus period (also averaged across three trials).

High gamma responses were extracted from raw downsampled recordings by further bandpass filtering (70-140 Hz) using a digital zero-order 6rd order Butterworth filter. Next, signals were rectified and smoothed with a 20 ms sliding window. Resulting signals that exceeded 5 times the 90th percentile were interpolated. Evoked high gamma magnitudes were extracted as for ERPs.

Estimation of best frequency

All analyses of tone-evoked responses were restricted to the range of 1.4-32 kHz tones. Best frequency was estimated by computing the center of mass of tone-evoked responses at 70 dB SPL. The response mass function was defined by the mean vector after projecting all responses on a circular domain where vector angles are represented by tone frequencies, to prevent biasing the center of mass towards the interior of the 1.4-32 kHz stimulus range.

Principal component analysis (PCA)

Evoked responses were analyzed by including both temporal (i.e., *R* post-stimulus responses) and spatial (i.e., *S* responsive sites) variables. These measurements were concatenated across individual trials, *T*, to create a 2-dimensional *T* (rows) x *R*-*S* (columns) matrices. PCA was then performed and *R*-*S* vectors were compressed using singular value decomposition to obtain a reduced-rank approximation of the original matrix. PCA was also performed on variations of our data including only spatial *P* values (i.e., including only evoked magnitudes) or only temporal *R* values (i.e., averaging responses across all recording sites). The top 15 ranked projections were preserved for further analysis, reducing the datasets into a *T* (rows) x 15 (column) matrix.

Tensor component analysis (TCA)

We applied a canonical polyadic (CP) decomposition to a 3-dimensional model, enabling us to treating spatial and temporal aspects of iEEG recordings across multiple trials as linear independent (orthogonal) dimensions (Kolda and Bader, 2009; Williams et al., 2018). Naive feature vectors were constructed by arranging all data into a three-dimensional matrix composed of length-*R* post-stimulus responses, *S* responsive sites, and *T* stimulus trials resulting in a *R* x *S* x *T* matrix. CP decomposition was performed (Bader et al., 2023) for 15 latent factors, the number 15 chosen to exceed the number of tone or implant stimuli and to parallel the data reduction performed by PCA. Then the resulting estimate of the *T* factors for each of the 15 components reduced our datasets into *T* (rows) x 15 (column) matrices.

Linear discriminant analysis (LDA)

We trained a decoder for predicting stimulus identity from single trial recordings by developing a supervised linear classifier. Each decoder was retrained and retested 1,000 times to average decoder performance across randomizations for combinations of trials used for training and test sets. Specifically, each bootstrap replicate was randomly partitioned to include 13 trials per stimulus for each training set and the remaining trials being used to test the decoder. LDA was applied to estimate the stimulus-likelihood map of the PCA– or TCA-compressed feature space. Naive feature vectors from the training set were normalized and compressed according to the learned transformations, and the maximum likelihood stimulus (i.e., the identity of the tone frequency or active cochlear implant electrode) was estimated for each response. Absolute accuracy of the decoder was computed as the average accuracy over all stimuli was estimated by the total proportion of correct predictions. In addition to absolute accuracy, we also computed the mean of the error distances between the predicted and actual stimulus, i.e., octaves or number of electrodes.

Linear mixed effects modeling

Group comparisons between normal-hearing and cochlear implant conditions were assessed using linear mixed-effects (LME) models implemented in MATLAB (fitglme, MathWorks). For each analysis, the dependent variable was modeled with at least fixed effects of condition (normal-

hearing vs cochlear implant) and a random intercept for animal to account for repeated measurements within subjects. Model significance for fixed effects was evaluated using F-tests obtained from an ANOVA on the fitted LME model.

Results

iEEG recordings in normal hearing and cochlear implanted rats

We had two main goals: 1) to determine which features of auditory cortex iEEG signals were most informative about stimulus identities; and 2) to use iEEG recordings to assess cortical coding of acoustic vs electrical stimuli in normal-hearing (NH) vs bilaterally deafened + unilaterally cochlear implanted (CI) rats. Animals were first anesthetized and then a craniotomy was performed to expose the primary auditory cortex. We implanted a custom 60-channel iEEG recording array (Insanally et al., 2016; Trumpis et al., 2017) over primary auditory cortex. Seven rats were normal-hearing and presented with acoustic pure-tone stimuli (Fig 1A, 'NH'). Seven rats were bilaterally deafened via cochleostomy before receiving a unilateral cochlear implant (Fig. 1B, 'CI'). Peripheral sensitivity and tuning were assessed using electrically evoked compound action potentials (ECAPs), recorded via implanted channels. Using a forward masking paradigm (Azadpour et al. 2022) we found cochlear implant stimuli were consistently tuned, cochleotopically and temporally (Supplemental Fig. 1).

A subset of these animals from each of the two groups (N=4 normal-hearing rats, N=3 cochlear implant rats) were trained on an auditory detection and recognition go/no-go task we have used previously, both for normal hearing (Froemke et al., 2013; Carcea et al., 2017; Insanally et al., 2024) and with cochlear implants (King et al., 2016; Glennon et al., 2023). Normal-hearing rats each achieved high levels of performance, whereas the cochlear implant rats had more variable performance (Fig. 1C; normal-hearing behavioral performance d': 2.9±0.1, cochlear implant performance: 0.9±0.2, one normal-hearing animal lost the implant prior to that stage of training).

The combinations of animals that underwent behavioral training and acute iEEG measurements are shown in Supplemental Fig. 2. We acquired and then compared acute iEEG recordings of acoustic tone-evoked and electrical cochlear-implant-evoked responses in normal-hearing and cochlear implant rats. Raw responses were down-sampled and lowpass filtered to eliminate electrical artifacts from cochlear implant stimuli, and bandpass filtered again either to reveal slowly varying event-related potentials (ERPs, bandpass range: 2-100 Hz) or to reveal higher frequency high gamma oscillations (HG, bandpass range: 70-140 Hz) (Fig. 1D). Trial-averaged evoked responses were time-locked to the stimulus onset. Evoked response magnitudes were not measurably different between normal-hearing and cochlear implant rats (Fig. 1E). We found that the behavioral training (denoted purple in all figures) had no measured effect on our analyses of sensory encoding compared to responses measured in untrained rats (linear mixed effects model, $p>0.3$ comparing normal hearing and cochlear implant signals in untrained vs trained rats).

A1 encoding of tones and cochlear implant electrodes are spatially organized

iEEG recordings of tone-evoked responses are spatially restricted to areas across the recording array that appeared to shift as a function of tone frequency in normal-hearing animals (Fig. 2). Determining the best frequency at each recording site (i.e., the stimulus evoking the maximum response overall at that location) confirmed the general tonotopic organization of auditory cortex (Fig. 2A-E, ERPs; Fig. 2F-J, HG). Tone-evoked responses were similar in expected directions and gradients (Polley et al., 2007) indicating that iEEG measurements have the spatial resolution for testing whether evoked responses are cochleotopically organized.

We then asked whether central auditory pathways would effectively preserve cochleotopic encoding provided by acute cochlear implants. We found that iEEG recordings of responses evoked by individual electrodes were spatially restricted to areas across the recording array (Fig.

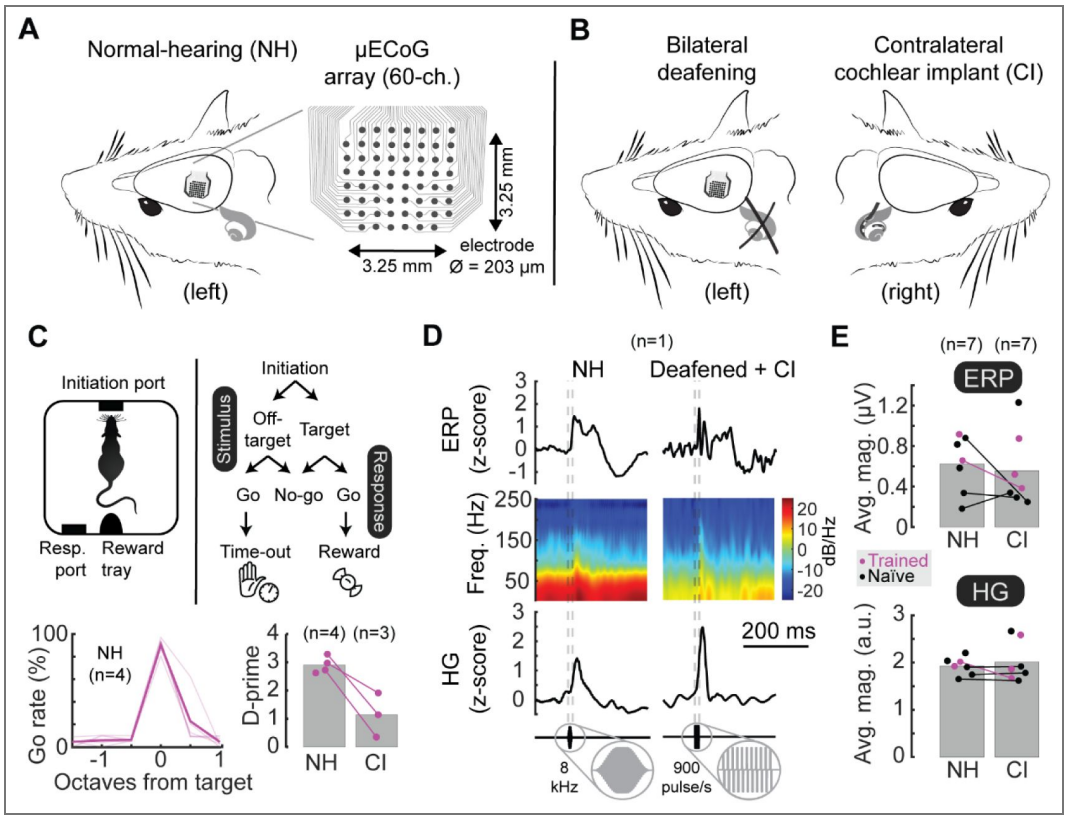

Figure 1. Auditory cortex iEEG responses to pure tone stimuli in normal-hearing and deafened cochlear implant rats.

A, Schematic of 60-channel cortical surface electrode arrays, covering 3.25 x 3.25 mm on the surface of auditory cortex to record tone-evoked responses in normal-hearing (NH) trained rats. **B**, Some animals were bilaterally deafened and fitted with a unilateral cochlear implant (CI). **C**, Behavioral training of subset of animals on auditory go/no-go frequency recognition task. Animals were first trained when normal-hearing (NH, N=4, d': 2.9±0.1) and then re-trained to respond to cochlear implant stimulation (CI, N=3, d': 0.9±0.2). **D**, Examples of trial-averaged single-site iEEG responses (top, ERPs; middle, ERP spectrograms; bottom, HG). Clear transients were evoked by tones in normal-hearing animals (NH, left column) and in cochlear implant rats (CI, right column). **E**, iEEG response magnitude was similar between normal-hearing (NH, ERP amplitude: 1.9±0.1 μV; HG amplitude: 0.6±0.1 a.u.) and cochlear-implant rats (CI, ERP amplitude: 2.0±0.2 μV, p=0.53 compared to normal-hearing ERPs, linear mixed effects; HG amplitude: 0.6±0.1 a.u., p=0.39 compared to normal-hearing HG).

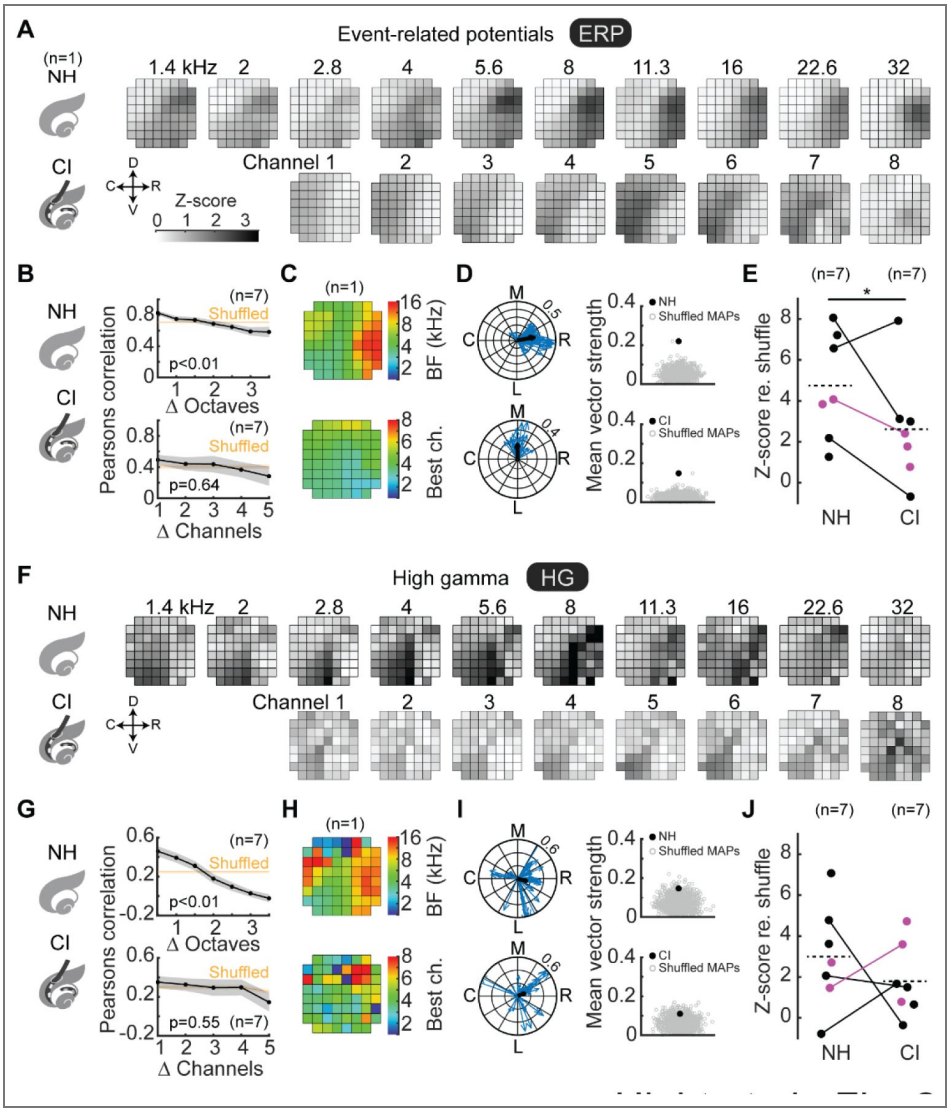

Figure 2. Tone-evoked and cochlear implant-evoked iEEG measurements are spatially organized.

A, F, Trial-averaged tone-evoked event-related potentials (ERPs, panel **A**) and high gamma (HG, panel **F**) were spatially restricted to regions along the iEEG recording array; these active regions shifted as a function of stimulus. **B, G**, Spatial correlations of evoked response areas decreased monotonically as a function of increasing stimulus separation, truncated at large separations due to low sample sizes. Evoked iEEG responses as assessed by ERPs and HG were nonrandom for normal-hearing and implanted rats ($p<10^{-8}$ compared to all shuffled responses), but were locally tonotopic in normal-hearing rats ($p<10^{-4}$) but not implanted rats (ERPs: p=0.5, HG: p=0.7). **C, H**, Determining the preferred stimulus of spatially-evoked activity revealed smooth gradients shifting from high-to-low to high tone frequencies or cochlear implant channels (ERPs, panel **C**; HG, panel **H**). **D, I**, Local tonotopic gradients for each recording site plotted on a unit circle (blue) as a function of magnitude (strength of gradient) and angle (direction of gradient). The vectors across each recording site were averaged to produce an overall tonotopic vector (black) whose magnitude represents a metric of overall topography (ERPs, panel **D**; HG, panel **I**). The mean vector was plotted against the mean vector computed from n=1,000 shuffled maps (ERPs, panel **D**: normal-hearing z-score: 6.6, $p<10^{-10}$; implanted z-score: 7.9, $p<10^{-14}$; HG, panel **I**: normal-hearing z-score: 2.1, p=0.02; implanted z-score: 1.5, p=0.07). **E, J**, Z-scored magnitudes of mean tonotopic vectors across animals (ERPs, panel **E**: normal-hearing mean z-score: 4.7±1.0, implanted mean z-score: 2.6±1.0, p=0.05, linear mixed effects; HG, panel **J**: normal-hearing mean z-score: 3.0±0.9, implanted mean z-score: 2.1±0.9, p=0.48).

2A,F) that appear to shift as a function of cochlear electrode location. To determine the degree of local and longer-range topography, we computed the spatial correlations as a function of stimulus separation, and compared the actual correlation coefficients to the distribution of responses when spatial locations were randomly shuffled. This analysis revealed a spatially structured but relatively coarse topographic organization that was non-random (Fig. 2B,G; $p<10^{-8}$ compared to all shuffled responses for ERPs and HG both for normal-hearing and implanted rats), but less sharply tonotopic relative to the tonotopic organization in normal-hearing animals assessed with pure tones (Fig. 2B, $p<10^{-4}$ for ERPs and HG for normal-hearing rats; Fig. 2G, ERPs: p=0.64, HG: p=0.55 for implanted rats). At the extremes, the spatial correlations were always higher for small vs. large tone separations (NH 0.5 vs ≥3.5 octaves, ERP: $p<10^{-4}$, HG: $p<10^{-4}$ Student's one-tailed t-test) and electrode separations (CI 1 vs ≥5 electrodes, ERP: p=0.01, HG: p=0.04).

We then reduced stimulus-evoked responses into representative stimulus maps (Fig. 2C,H) whose areas and orientations of these maps qualitatively match those published from similar iEEG recordings (Insanally et al. 2015), and single unit recordings (Polley et al, 2006) albeit at coarser gradients likely due to aggregate recordings of excitatory and inhibitory activity and spatial low-pass filtering due to potentials originating far from recording sites. Direct within-animal comparisons of normal-hearing vs implant maps (N=4) indicated that cochleotopic gradients were positioned in similar orientations and directions (Fig. 2C,H, Supplemental Fig. 3). To quantify the degree and direction of potential spatial tonotopic or cochleotopic organization in the iEEG recordings, we computed the local gradients for each recording site (one example animal shown in Fig. 2D, ERPs; Fig. 2I, HG). Each gradient is a vector consisting of a magnitude and direction, and thus we then averaged these gradients from each recording site to get the overall cochleotopic vector, the magnitude of which is an index of spatial organization for a given animal (Romero and Hight et al. 2020). We shuffled the recording site location labels to generate putatively randomly organized maps (n=1000 random shuffles per animal), and compared the actual mean vector strength to the shuffled distributions. For this example animal, the ERP maps were significantly different from chance in terms of spatial organization (Fig. 2D, NH p=0.00003, CI p=0.0033), while this was more modest for the HG maps in this animal (Fig. 2I, NH p=0.02, CI p=0.07). This analysis revealed a similar kind of organization between ERP and HG maps of normal-hearing vs cochlear implant rats (Fig. 2E, NH mean z-score: 4.7±1.0, CI mean z-score: 2.6±1.0, p=0.05 linear mixed effects; Fig. 2J, NH mean z-score: 3.0±0.9, CI mean z-score: 2.1±0.9, p=0.49). Combined with results from Figure 2B,G, these analyses indicate that overall there was similar spatial organization to cortical iEEG responses in normal-hearing and cochlear implant animals, although the organization was substantially coarser and less sharply resolved in cochlear implant animals..

Increased variability of trial-by-trial responses evoked by cochlear implant stimulation

The results described above for Figures 1 and 2 used trial-averaged responses to examine the spatio-temporal organization of iEEG responses. We noticed that the iEEG recordings provided satisfactory signal-to-noise ratios to measure evoked ERPs (Fig. 3A,B) and HG transients (Fig. 3C,D) on a single trial basis. Therefore, we next asked if there were differences in single-trial encoding for cochlear implant vs normal-hearing rats. We first averaged evoked responses across all recording sites to reduce measurement noise. We then computed variability of responses in the 50 ms period immediately following stimulus onset, and found that in this temporal domain, the within-animal trial-by-trial variability in evoked responses was similar for cochlear implant rats compared to normal-hearing rats irrespective of recording site ('Temporal'; Fig. 3B, ERPs, linear mixed effects, p=0.054; Fig. 3D, HG, p=0.17).

Then, we returned to the evoked responses for each recording site and measured the trial-by-trial evoked response peak. Next, we computed the variability of spatial distributions of evoked responses and found modestly larger within-animal trial-by-trial variability in the spatial domain of ERP responses for CI compared to normal-hearing rats ('Spatial'; Fig. 3B, ERPs, linear mixed effects model, p=0.01; Fig. 3D, HG, p=0.35). Differences were subtle but consistent across animals

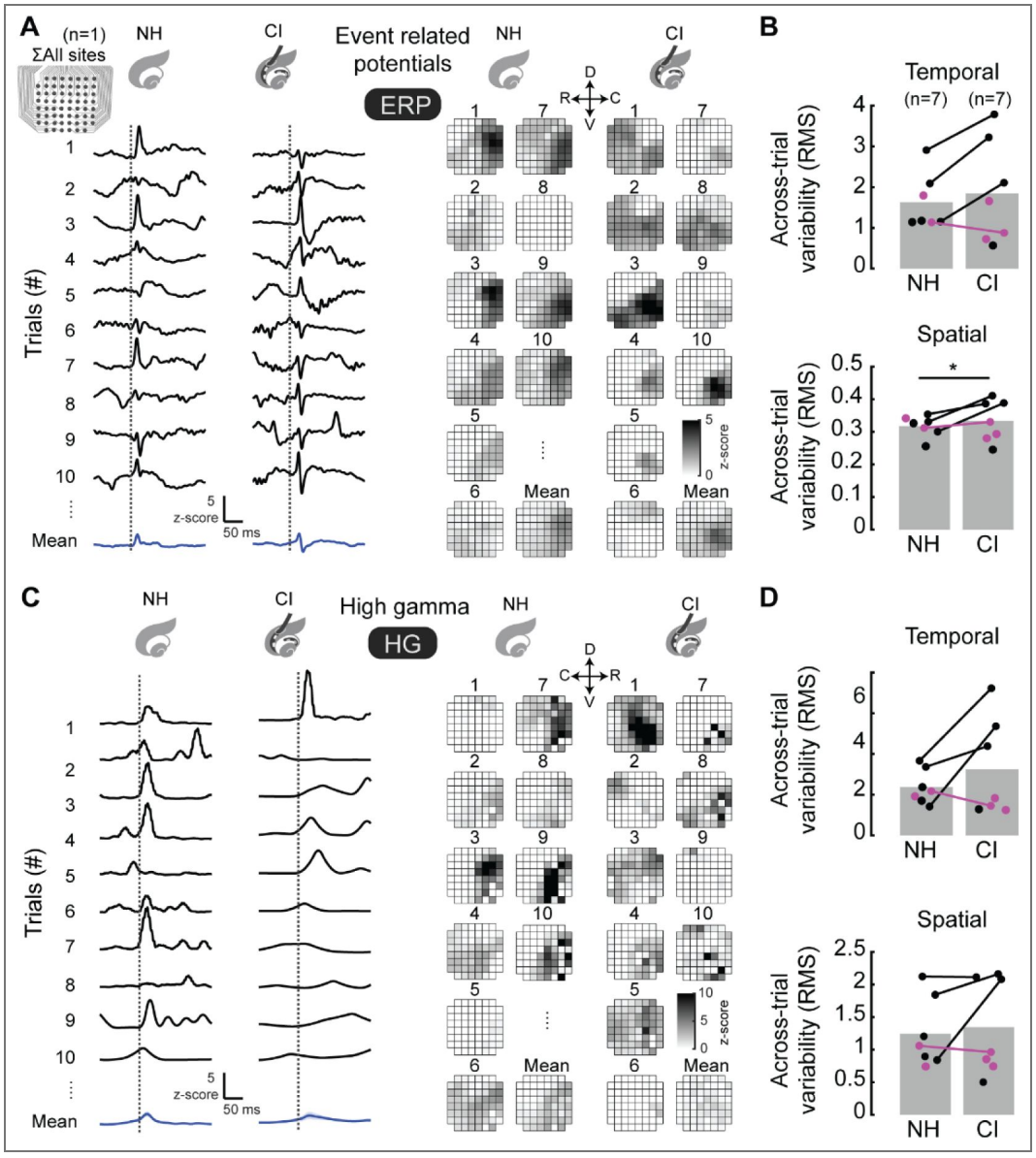

Figure 3. Trial-by-trial cochleotopic encoding is more variable in cochlear implant vs normal-hearing rats.

A, C, Trial-by-trial evoked iEEG measurements in both normal-hearing and implanted rats revealed peaks across time (left) and space (right) (ERP, panel **A**; HG, panel **C**) **B, D,** Variability of iEEG measurements across trials (root mean square, rms) was consistently higher for spatial distributions of cochlear implant-evoked compared to tone-evoked activity, for ERPs in panel **B** (bottom, ERP spatial NH mean rms: 0.32±0.01, CI mean rms: 0.33±0.02, p=0.011, linear mixed effects) but not for temporal distributions (top, ERP temporal NH mean rms: 1.6±0.3 over all animals, CI mean rms: 1.9±0.5, for animals monitored before and after deafening, p=0.054) and HG in panel **D** (top, HG temporal NH mean rms: 2.4±0.3 over all animals, CI mean rms: 3.3±0.9, p=0.17; bottom, HG spatial NH mean rms: 1.2±0.2, CI mean rms: 1.3±0.3, p=0.35).

(Fig. 3B). We conclude that similar to the trial-averaged responses in Figure 2, analysis of ERPs more so than HG signals could identify the increased spatial variability of evoked responses across the auditory cortex in cochlear implant animals relative to normal-hearing rats.

Single trials encode stimulus identity in normal-hearing and cochlear implant rats

Given that trial-by-trial variability was higher for implant-evoked responses vs responses in normal-hearing rats, we wondered if this compromised decoding of cochlear implant signals in some way. We next trained a classifier to ask if we could successfully decode stimulus identity from individual trials, and examine differences of decoding accuracy for normal-hearing vs cochlear implant rats. We reduced evoked responses into the top 15 principal components via PCA (Fig. 4A,B). The number of components (15) was chosen based on PCA scree plots (Supplemental Fig. 4A), which showed that explained variance entered a near-linear, low-slope regime beyond this point demonstrating a similar plateau in reconstruction error (Supplemental Fig. 4B), indicating diminishing returns for additional components. We then trained an LDA decoder on 13 randomized trials of stimulus presentation to enable comparisons across animals that had different numbers of stimuli (Insanally et al., 2016). Computed prediction probabilities were estimated by testing the decoder on the remaining trials. Selections of the 13 training and remaining test trials were randomized (N=1,000 trials), and final prediction probabilities averaged across repeats.

This approach successfully decoded tones and implant electrodes (Fig. 4C). Across rats, there were above-chance predictions of correct stimuli from single trials, with higher errors when closer to the actual stimulus (Fig. 4D). Computing error distance mean across trials allowed us to compare decoding performance of normal-hearing vs implanted rats, as this combines absolute prediction probability and distribution of errors while normalizing to chance-level error distances, determined by number of trained and tested stimuli. Decoders trained on responses from normal-hearing rats performed better compared to responses after implantation (Fig. 4E; ERP mean error distance for normal-hearing rats: 0.74±0.05, cochlear implant rats: 0.78±0.06, $p<10^{-4}$, linear mixed effects; HG mean error distance for normal-hearing: 0.90±0.03, cochlear implant: 0.91±0.04, p=0.15).

Single trial encoding is independently provided by both spatial and temporal cues

Which aspects of iEEG signals (spatial topography and/or temporal dynamics) contribute to stimulus decoding performance? We re-trained PCA-LDA decoders, but instead of using both spatial and temporal aspects of the full set of iEEG measurements (Fig. 5A), decoders were trained on the spatial-only (Fig. 5B) or temporal domain-only aspects (Fig. 5C) of evoked iEEG measurements. Decoders trained on the spatial or temporal domains only were essentially as good as predicting the stimulus as decoders trained on both aspects (Fig. 5D,E; mean error distance for spatial-only ERPs, normal-hearing: 0.77±0.04, implant: 0.77±0.08; for spatial-only HG, normal-hearing: 0.89±0.04, implant: 0.87±0.05; for temporal-only ERPs, normal-hearing: 0.82±0.05, implant: 0.81±0.07; for temporal-only HG, normal-hearing: 0.87±0.04, implant: 0.93±0.05; for spatial+temporal ERPs, normal-hearing: 0.74±0.04, implant: 0.86±0.06; for spatial+temporal HG, normal-hearing: 0.90±0.03, implant: 0.97±0.04). We conclude that both spatial and temporal aspects of iEEG measurements contribute to single-trial encoding of stimulus identity.

In some cases, we found that the performance of either spatial-only or temporal-only could be somewhat better than decoders trained on both spatial and temporal aspects of iEEG measurements. This is likely due to the noise inherent in iEEG signals, such that constraining PCA reductions to one aspect of the data (either spatial or temporal) helps to eliminate variance in individual recordings.

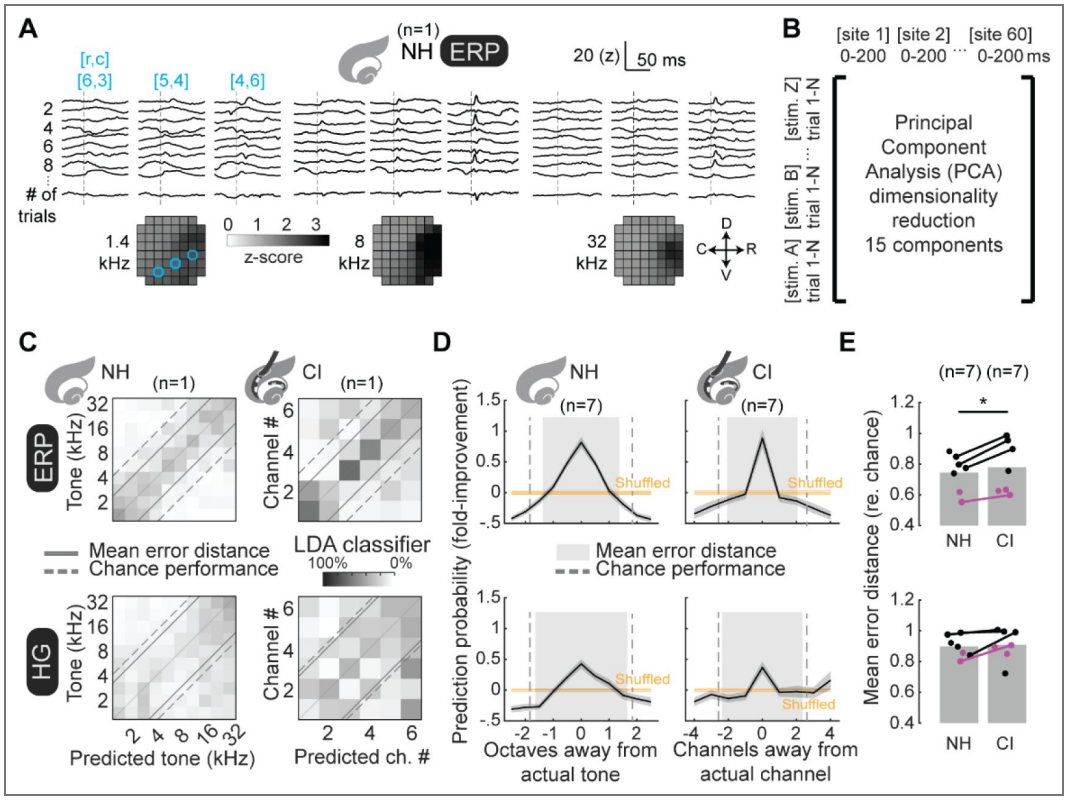

Figure 4. Trial-by-trial iEEG measurements encode stimulus identity.

A, Trial-by-trial ERPs evoked by 1.4 kHz (left), 8 kHz (middle), and 32 kHz tones (right) are plotted for three recording sites (blue) reveal discernable evoked transients and spatially restricted patterns of evoked magnitudes (stimulus onsets depicted by dotted line). **B,** Trial-by-trial iEEG measurements concatenated such that columns represent recording sites (spatial) and post-stimulus sampling (temporal), rows by stimulus trials. Data then reorganized by PCA and reduced to the 15 components according to magnitude of explained variance. **C,** Classification matrices are plotted means across bootstrapped repeated (N=1,000) versions of LDA classifiers trained using 13 randomly selected trials for each stimulus, and classification predictions of single and remaining trials reveal significant prediction of stimulus identity (dashed line: chance-level error distance; solid lines: actual mean error distances). **D,** Stimulus prediction probabilities plotted across animals (black: mean, grey: s.e.m.) and as function of either octaves (normal-hearing) or channels (cochlear implant) from actual stimulus, reflecting a gradient in which adjacent stimuli share more encoded features than other stimuli. **E,** Decoder performance (mean error distance) across individual animals was somewhat worse for cochlear implant ERPs compared to tone-evoked ERPs (ERP mean error rate relative to chance for normal-hearing: 0.74±0.05, cochlear implant: 0.78±0.06; for animals assessed both first when normal-hearing and then after cochlear implantation $p<10^{-4}$, linear mixed effects), but not for HG (HG mean error rate relative to chance for normal-hearing: 0.90±0.03, cochlear implant: 0.91±0.04; for animals assessed both first when normal-hearing and then after cochlear implantation p=0.15).

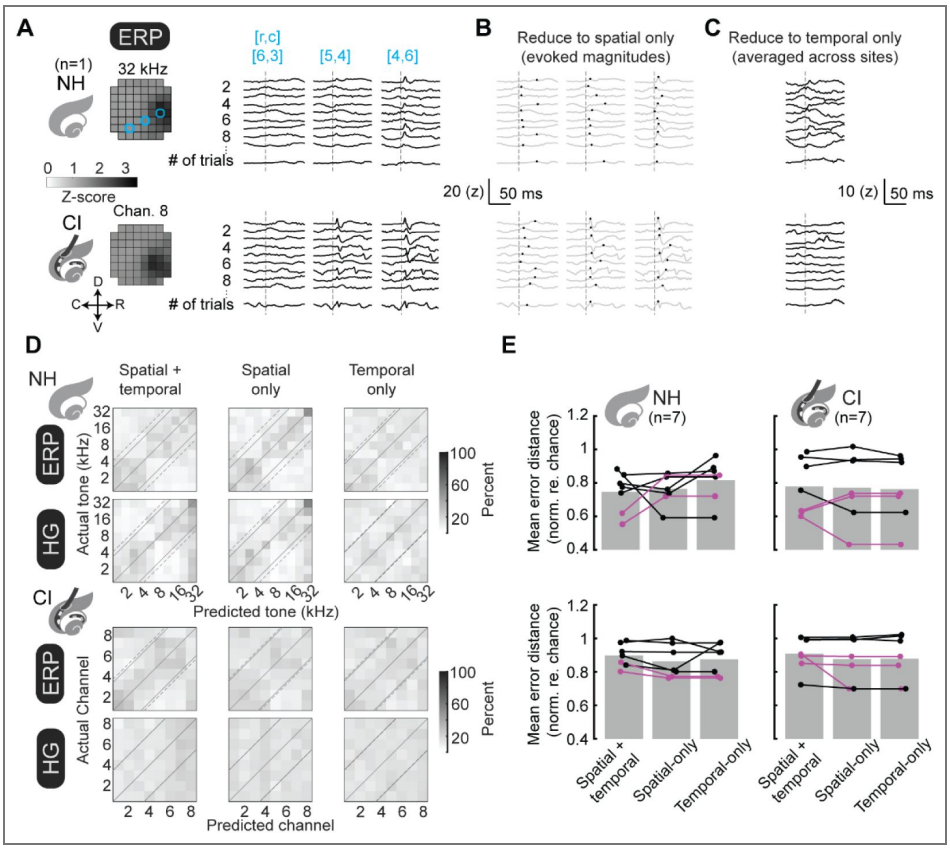

Figure 5. Trial-by-trial decoding from either spatial or temporal aspects of iEEG signals.

A, Raw trial-by-trial ERPs for a single animal are plotted for 3 channels. **B-C,** Trial-by-trial iEEG measurements are reduced into either spatial only (**B**) or temporal only (**C**) by extracting either the magnitude of evoked activity or averaging across all recording sites. **D,** Re-training PCA-LDA decoders on spatial-only (middle) or temporal-only (right) does not abolish the encoding of stimulus identity. **E,** Decoder errors (mean error distance re. chance) across animals are plotted for decoders trained on spatial+temporal, spatial-only, and temporal-only iEEG measurements. Mean error distance for spatial+temporal ERPs, normal-hearing: 0.74±0.04, implant: 0.86±0.06; for spatial+temporal HG, normal-hearing: 0.90±0.03, implant: 0.97±0.04. Mean error distance for spatial-only ERPs, normal-hearing: 0.77±0.04, implant: 0.77±0.08; for HG, normal-hearing: 0.89±0.04, implant: 0.87±0.05. Mean error distance for temporal-only ERPs, normal-hearing: 0.82±0.05, implant: 0.81±0.07; for HG, normal-hearing: 0.87±0.04, implant: 0.93±0.05.

Reducing evoked responses using TCA preserves encoding of stimulus identity

One challenge with using PCA is that the ordinations of dimensionality reduction are unconstrained, because they are arbitrary linear combination of the original variables. A newer approach for dimensionality reduction called tensor component analysis (TCA) explicitly enables identification of which spatial, temporal, and single-trial factors best account for signal variability, and thus drive single-trial stimulus decoding (Williams et al., 2018). Here, we used TCA instead of PCA for LDA-based decoding, constraining data reduction dimensions on the full data set to the spatial, temporal, and to the trials of iEEG measurements (Fig. 6A). The resulting TCA-optimizations across 15 components reveal discernable patterns of spatial and temporal factors (Fig. 6B). We trained and tested a LDA decoder using only the trial factors, and found that single trial predictions accurately identified the stimulus (Fig. 6C-D). Decoders trained on responses from normal-hearing rats had better prediction performance compared to the responses from these same animals after cochlear implantation (Fig. 6E; ERP mean error distance for normal-hearing rats: 0.78±0.04, for cochlear implant rats: 0.80±0.06, $p<10^{-5}$, linear mixed-effects model; HG mean error distance for normal-hearing: 0.90±0.03, for cochlear implant: 0.88±0.05, p=0.03).

Latent factors from unsupervised TCA revealed spatially-organized maps

These analyses revealed that single-trial iEEG responses can be successfully decoded, and the TCA-based approach suggests that individual factors driving decoding might relate to specific spatiotemporal features inherent in the data. Specifically, we asked whether the TCA-reduced data contained organized spatial features, e.g., patterns of tonotopy. We next optimized TCA models of the original data (Fig. 7A) and then weighed the spatial factors by the strength of trial factors associated with each stimulus, resulting in spatial maps for each stimulus frequency for both normal-hearing and electrode for implants rats (Fig. 7B). The resulting reorganized spatial factors were further reduced to a preferred stimulus. Resulting TCA-maps exhibited tonotopic features (Fig. 7C), similar to tonotopic maps extracted from ERP or HG components of the iEEG responses. TCA-recreated spatial maps also exhibited coarse topographic organization that was non-random compared to shuffled distributions (Fig. 7D, $p<10^{-8}$ compared to all shuffled responses for ERPs and HG both for normal-hearing and implanted rats). TCA models from normal-hearing HG iEEG measurements exhibited clear tonotopic organization whereas tonotopy in models from other measurements was less clear (Fig. 7D, normal-hearing rats ERPs: p=0.18, normal-hearing rats HG: $p<10^{-4}$, cochlear implant rats ERPs: p=0.43, cochlear implant rats HG: p=0.40). As with analyses of Figure 2E,J, the magnitude of tonotopy computed from mean vector strengths was similar for ERP and HG measurements in normal-hearing vs cochlear implant rats (Fig 7E).

iEEG measurements from implanted rats could not be decoded from models trained on normal-hearing data

We asked what features might be shared vs distinct in the nature of cortical encoding of tones (in normal-hearing rats) and electrode channels (in cochlear implant rats). We hypothesized that this overlap would be incomplete, with substantial variability across individuals. This was based on a considerable number of previous studies finding that adaptation periods are needed before maximizing cochlear implant outcomes in both animals (Glennon et al., 2023) and humans (Holden et al., 2013; Cusumano et al., 2017; Glennon et al., 2020; Caswell-Midwinter et al., 2022), as well as our results described above showing that iEEG measurements were less sharply topographic and more variable in implanted rats compared to normal-hearing animals. Thus, here we asked whether a decoder trained on tone-evoked iEEG measurements from normal-hearing rats could interpret implant-evoked iEEG measurements on single trials.

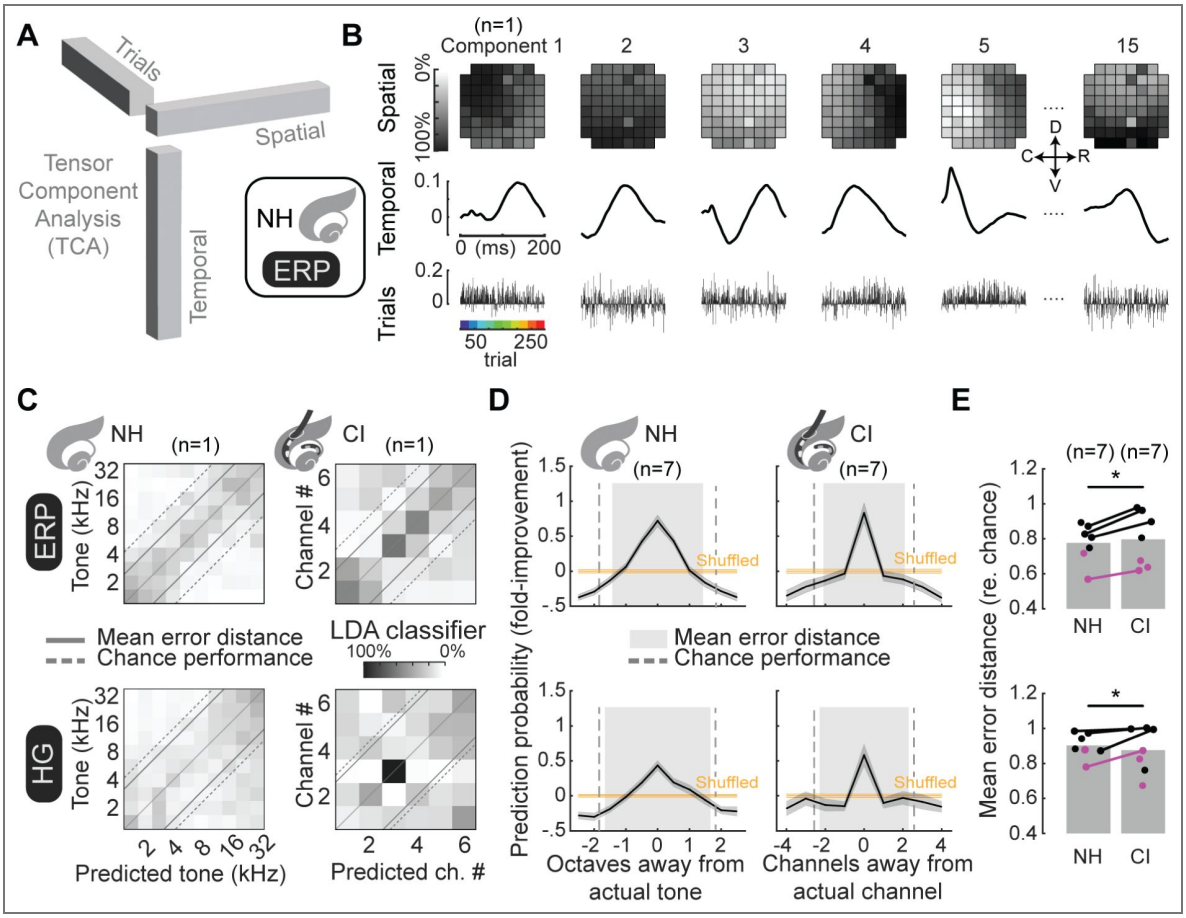

Figure 6. TCA-based decoding of single-trial iEEG measurements.

A, Schematic of TCA with 3-dimensional tensors with orthogonal dimensions of spatial, temporal and trial factors. **B,** TCA-reduced iEEG measurements of stimulus-evoked ERPs in normal-hearing rats are plotted across 15 components of spatial (top row), temporal (middle row) and trial factors (bottom row). **C,** Classification matrices of mean decoder predictions across bootstrapped repeated (N=1,000) versions LDA classifiers trained using 13 randomly selected trials for each stimulus indicated that iEEG measurements encode stimulus identity from single stimulus presentations (dashed line: chance-level error distance; solid lines: actual mean error distances). **D,** Stimulus prediction probabilities are plotted across animals (black: mean, grey: std. error) and as a function of either octaves or channels in away from actual stimulus, normal-hearing and implanted rats. Correct prediction probabilities are high across all conditions and prediction errors coalescing of predictions toward actual stimuli (orange: mean and std. error of decoder performance on shuffled trials; grey: mean error distance, dashed line: chance level error distance). **E,** Decoder errors (mean error distance) across individual animals were slightly smaller for evoked iEEG measurements in normal-hearing compared to implanted rats (ERP mean error rate re. chance normal-hearing: 0.77±0.04, implanted: 0.80±0.06; HG mean error rate re. chance normal-hearing: 0.90±0.03, implanted: 0.88±0.05). Comparisons between normal-hearing and implanted iEEG measurements showed significant decrease in estimated error distances for ERP (top, linear mixed-effects model: $p<10^{-5}$) and HG (bottom, p=0.03).

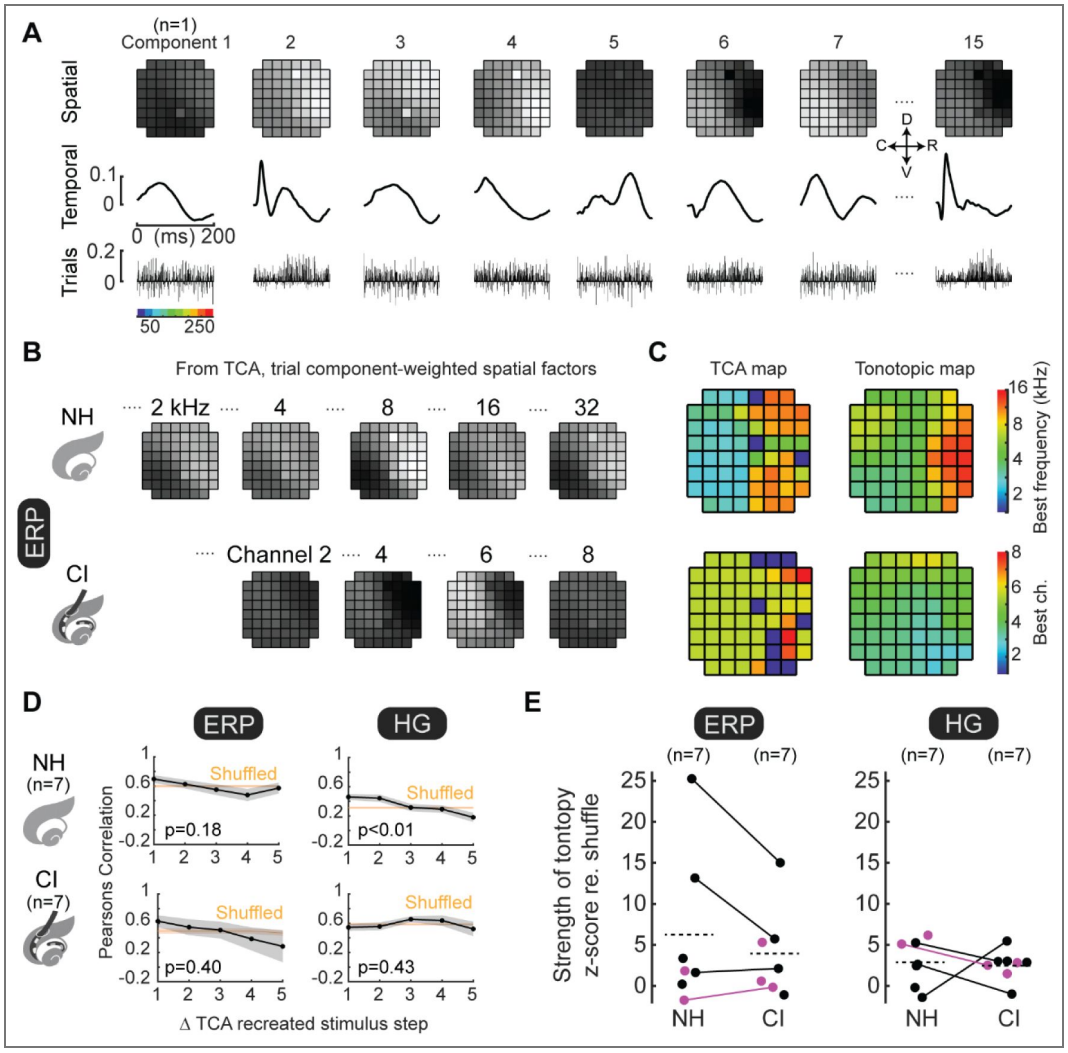

Figure 7. TCA data reductions reveal latent spatial factors are topographically organized.

A, TCA-based analysis of evoked neural activity, divided into 15 unique components where each component is separated into orthogonal dimensions of spatial factors (top row), temporal factors (middle row) and trial factors (bottom row). **B**, Spatial maps for tone-evoked or electrode-evoked responses recreated from TCA reduced data. **C**, Reducing re-organized spatial factors revealed a TCA map (left) with topographical gradients in same location and direction as the tonotopic map reduced from raw measurements (right). **D**, Spatial correlations of evoked response areas decreased monotonically as a function of increasing stimulus separation. TCA-reduced models of evoked iEEG responses as assessed by ERPs and HG were nonrandom for normal-hearing and implanted rats ($p<10^{-8}$ compared to all shuffled responses). TCA-reduced models were locally tonotopic only for HG in normal-hearing rats (normal-hearing ERPs: p=0.18, normal-hearing HG: $p<10^{-4}$, cochlear implant ERPs: p=0.43, cochlear implant HG: p=0.40). **E**, Z-scored magnitudes of mean tonotopic vectors across animals were similar (ERPs, normal-hearing mean z-score: 6.2±3.6, cochlear implant mean z-score: 3.9±2.1, p=0.16, linear mixed effects; HG, normal-hearing mean z-score: 2.9±1.1, implanted mean z-score: 2.5±0.7, p=0.75).

Our measurements of iEEG activity in the same animals before and after deafening and implant fitting provide an opportunity to examine this directly, and determine how individually distinct the neural coding of sound is for the auditory cortex in both normal-hearing and cochlear implant conditions. TCA-generated models provide a reasonable approach to quantify the degree of information transfer from the normal-hearing to the implanted condition, because the dimensions of data reductions are predetermined (i.e., spatial and temporal), rather than unconstrained as with PCA models. We generated TCA models of tone-evoked iEEG measurements from normal-hearing rats (Fig. 8A). Next, we extracted only the spatial and temporal components of these normal-hearing TCA models to constrain models for implanted rats, leaving only the trial factors to be optimized (Fig. 8E).

Next, we compared these models across each animal by training an LDA decoder on the trial factors from tone-evoked TCA models and then testing the decoder on trial factors of the implant-evoked TCA models (Fig. 8F). From these resulting confusion matrices of prediction probabilities, we computed the mutual information between predictions of tone identity and actual implant channels to quantify how much tone predictions can be used to determine the actual identity of single channels, without imposing any hypotheses about how predicted tones map onto implant electrodes (e.g., tonotopy). We computed the pointwise mutual information for each combination of predicted tones and actual implant channels, which was then normalized by the joint probability. These resulting bits were combined across the entire confusion matrix to compute mutual information, and finally we converted this to a percentage of information transfer by dividing the experimentally measured mutual information by the total possible number of bits the matrix could provide.

We found the resulting information transfer to be low across all four animals where we measured both tone– and implant-evoked iEEG measurements (Fig. 8G; mean information transfer, ERPs: 1.2±0.6%; HG: 0.2±0.1%). The near-zero information transfer indicates that decoders trained on tone-evoked iEEG measurements do not make meaningful interpretations of implant-evoked iEEG measurements. We repeated this analysis but with first optimizing TCA models on a subset of tone-evoked data and then constraining the spatial and temporal factors while optimizing a new TCA model of withheld tone-evoked iEEG measurements (Fig. 8B). Training a classifier on the original and testing the re-optimized trial factors, we found above-chance decoding accuracy and stimulus tuning (Fig. 8C,D) indicating this analysis approach is effective. We conclude that although iEEG responses can be meaningfully decoded from single-trial cortical responses (to either acoustic tones in normal-hearing animals or cochlear implant stimulation in deafened animals), the decoding algorithms and computations required are specific to the type of stimulus and do not immediately generalize between acoustic and electrical stimulation. This has implications for understanding the perceptual experiences of cochlear implant users at acute implant stimulation. If the cortical representations were simply degraded or noisy versions of acoustic responses, we would expect partial information transfer. This was not observed. Instead, the mutual information analysis reveals that the acoustic response pattern does not inform the electrical stimulation response pattern. In turn, this suggests that the perceptual qualities (e.g., pitch) evoked by acoustic and electrical stimulation may be qualitatively different rather than simply degraded versions of each other.

Discussion

Cochlear implants are the gold standard for success of brain-computer interfaces and neuroprosthetic devices to safely activate the human nervous system and effectively restore functional sensation (Hochmair et al., 2006; Wilson and Dorman, 2008; Clark, 2015; Svirsky, 2017; Glennon et al., 2020). While high levels of hearing and speech processing can be achieved by some users, outcomes remain highly variable in terms of learning rates and peak performance, especially in real-world conditions and even after controlling for age and durations of deafness (Blamey et al., 2013). Invariably, all users require an adaptation period; speech perception outcomes are initially poorer than later timepoints (Holden et al., 2013; Cusumano et al., 2017; Caswell-Midwinter et al., 2022; Stronks et al. 2025), indicating both that acute

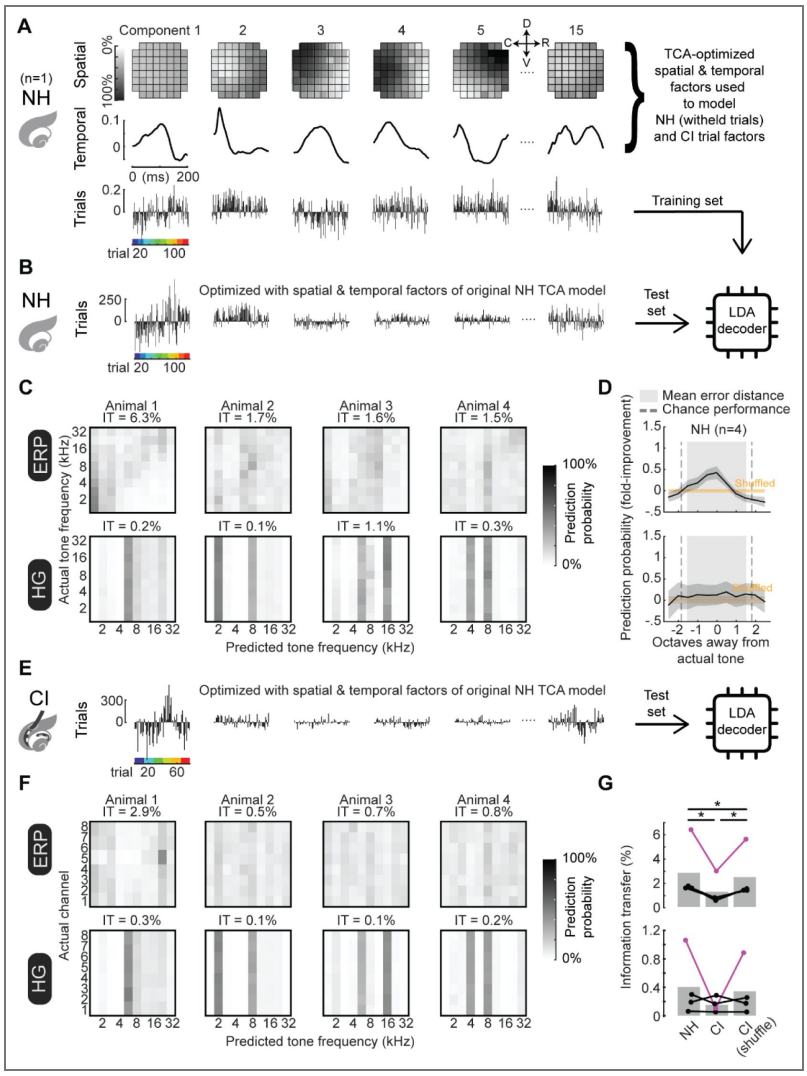

Figure 8. Lack of information transfer between acoustic and electrical stimulation representations in the same animals.

A, Evoked iEEG measurements from a subset of data from normal-hearing rat reduced using TCA. **B,** Evoked iEEG measurements from previously withheld trails from normal-hearing rat reduced using TCA, constraining the model with the spatial and temporal factors from the original TCA model, leaving only the trials as the optimizable variables. **C,** Linear discriminant analysis classifiers are trained on the trial factors extracted from the original TCA-reduced models of evoked data and then used to predict stimulus identity from the trial factors from the re-optimized TCA-reduced models of withheld normal-hearing measurements. **D,** Classification matrices are plotted means of decoder predictions across bootstrapped repeated (N=1,000) versions of linear-discriminant analysis (LDA) classifiers. Mutual information (IT) are indicated above these mean classification matrices. **E,** Stimulus prediction probabilities plotted across animals (black: mean, grey: s.e.m.) and as function of either octaves (normal-hearing) or channels (cochlear implant) from actual stimulus, reflecting a gradient in which adjacent stimuli share more encoded features than other stimuli (for ERP, but not HG). **F,** Evoked iEEG measurements in cochlear implant rat reduced using TCA, constraining the model with the spatial and temporal factors from the original TCA model optimized on normal-hearing data, leaving only the trials as the optimizable variables. Linear discriminant analysis classifiers are trained on the trial factors extracted from the original TCA-reduced models of evoked data in normal-hearing conditions and then used to predict stimulus identity from the trial factors from the TCA-reduced models of implant-evoked measurements. **G,** Classification matrices are plotted means of decoder predictions across bootstrapped repeated (N=1,000) versions of linear-discriminant analysis (LDA) classifiers. **H,** Information transfer of normal-hearing trained and implant tested decoders reveal little-to-no information transfer (IT mean across animals, ERP: 1.2±0.6, HG: 0.3±0.1%) compared to both normal-hearing (IT mean across animals, ERP: 2.8±1.2%, p=0.044, HG: 0.4±0.4%, p=0.187 one-tailed t-test) and cochlear implant where rows were shuffled within columns (IT mean across animals, ERP: 2.4±1.0%, p=0.042, HG: 0.3±0.2%, p=0.209, one-tailed t-test). Information transfer of normal hearing re-optimized decoders was significantly higher compared to cochlear implant decoders where rows were shuffled within columns (ERP: p=0.050, HG: p=0.107, Student's one-tailed t-test).

encoding of cochlear implant stimulation by the central auditory system is not optimal and that neuroplastic processes are needed for maximizing outcomes. Current and future advances in engineering and implant programming algorithms might help improve outcomes further, but there is a general belief in the field that what is now required is an understanding of how the central nervous system responds to peripheral electrical stimulation (Kral et al., 2002; Kral and Eggermont, 2007; Wilson and Dorman, 2008; Moore and Shannon, 2009).

Our findings provide the first direct neural evidence that acoustic and electrical cochlear stimulation create substantially distinct cortical representations, with near-zero information transfer between modalities. This addresses a longstanding question in cochlear implant research: whether electrical stimulation of the cochlea can evoke the same percepts as acoustic stimulation, such as pitch and timing. The lack of transferable representations suggests that cochlear implant users may experience qualitatively different percepts that cannot be predicted from normal acoustic hearing. If so, this would challenge a foundational assumption of current cochlear implant design—that electrical stimulation should mimic the tonotopic patterns of acoustic hearing. Our data suggest that this biomimetic approach may be fundamentally limited because the cortical representations are non-overlapping.

Previous studies in non-human animals have established that stimulus identity can be encoded in A1 (Bierer and Middlebrooks, 2002; Middlebrooks and Bierer, 2002; Bierer and Middlebrooks, 2004). However, many of these studies have used invasive recording methods to examine single-neuron responses to implant activation. Invasive recordings are not feasible for human cochlear implant recipients, and thus decoding methods based on purely-invasive measures may be difficult to translate into human subjects for optimizing implant programming and/or training for use of the device. While our iEEG recordings are also invasive and under anesthesia, the principles of iEEG analysis for cochlear implant responses developed here might be more applicable to non-invasive EEG recordings or similar approaches more easily performed in humans. Grid electrodes allowed us to take simultaneous advantage both of temporal and spatial features in the data, some of which were more obvious in ERPs, others were more latent in HG signals or PCA/TCA factors.

Our results show that these features could provide accurate stimulus decoding even on single trials, indicating that: 1) use of these methods in translational or clinical settings could aid personalization and optimization of brain-computer interfaces, and 2) single-trial implant responses can be adequately processed by auditory cortex and presumably downstream regions related to perception and behavior. It has been unclear to what degree the patterns of tone-evoked and implant-evoked responses in normal-hearing vs deaf subjects are similar. We found that the encoding of cochlear implant electrodes was less reliable and identifiable than tone-evoked responses in normal-hearing animals. One caveat is that direct comparisons of evoked iEEG measurements between normal-hearing and implanted rats are challenging due to fundamental differences in the stimuli (e.g., the cochleotopic separation between stimuli such as the spacing between half-octaves vs spacing between successive CI electrodes), as well as the higher degree of inter-trial variability for implant responses (which is presumably not influenced by stimulus separation).

We also observed interesting differences in the information provided by ERPs vs HG signals. In terms of field potentials, the HG band is thought to most directly related to neuronal spike activity (Ray and Maunsell, 2011), which may account for why HG-evoked activity was more time-locked to stimuli and more spatially tuned compared to ERPs. Some single-channel HG measurements also had higher signal-to-noise levels than ERPs. A priori, it would seem that a decoder with access to both higher signal-to-noise measurements in the temporal and spatial domains should perform better at predicting stimulus identity. Instead, we found that decoding was more accurate with ERPs than HG. One possible explanation for poorer decoding performance with HG is that HG signals are more spatially tuned, leading to a smaller number of discernable channels with clear HG activity; accordingly, we found that across iEEG grid sites, there were more significant

recording sites with ERPs than HG. HG responses also have higher trial-by-trial variability and are more temporally-constrained than ERPs, and thus the ERP might be more informative in terms of decoding performance.

Finally, we found that single-trial temporal factors could suffice to provide accurate decoding of implant channels. This suggests that preservation of clear cochleotopy in deaf subjects may not be a pre-requisite for successful implant use. Rather, it is likely that reductions in trial-by-trial and inter-neuronal variability might be more important as a mechanism for improving outcomes. This means that the neural responses to neuroprosthetic stimulation and use of brain-computer interfaces need not fully recapitulate responses to other modalities (e.g., acoustic stimulation) in space and time. These findings are consistent with the possibility that cochlear implant stimulation engages an alternative representation in auditory cortex, rather than a simple degraded version of acoustic encoding. Previously we showed that deafened rats could learn to use a cochlear implant to perform an auditory task, and that changes in cortical excitatory and inhibitory synapses related to implant use outcomes. In the current study, we did not track responses to implant use over time in relation to changes in perception and behavioral performance. Our results suggest that refinement particularly of inhibitory cortical responses might help increase inter-neuronal variance at the population level to increase spatial organization, while decreasing intra-trial variability at the single neuron level to enhance temporal organization and improve auditory perception.

Supplemental figures

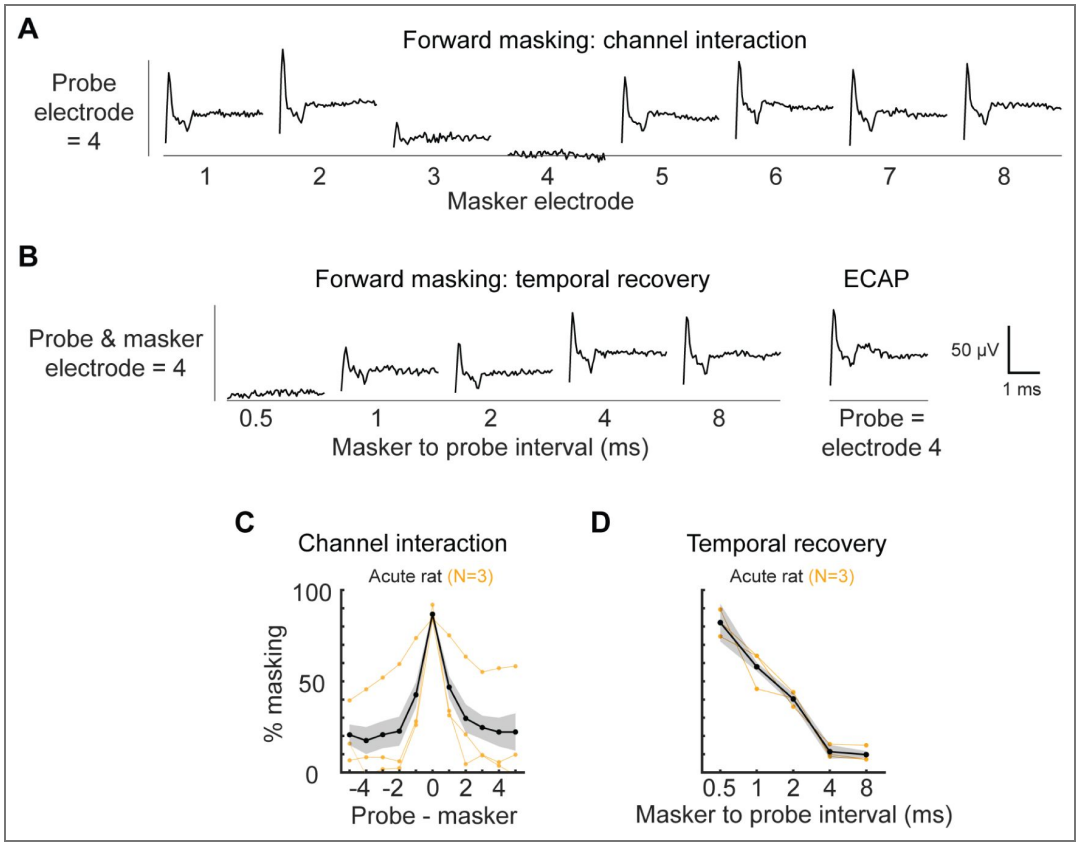

Supplemental Figure 1. ECAP measurements of spatio-temporal cochlear implant tuning. A, Forward masking was performed to assess the spatial tuning of cochlear stimuli in the cochlea via ECAPs measured by adjacent cochlear implant electrodes. **B,** Forward masking was performed to assess temporal tuning of cochlear implant stimuli in the cochlea via ECAPs measured by adjacent cochlear implant electrodes. The masker stimulus was delivered by the same electrode as the probe. **C,** Spatial tuning functions were averaged across all probe

electrodes in N=3 animals (black, mean; gray: s.e.m.; orange, average of individual subjects). **D,** Temporal tuning functions were averaged across all probe electrodes and N=3 animals (black, mean; gray, s.e.m.; orange, average of individual subjects).

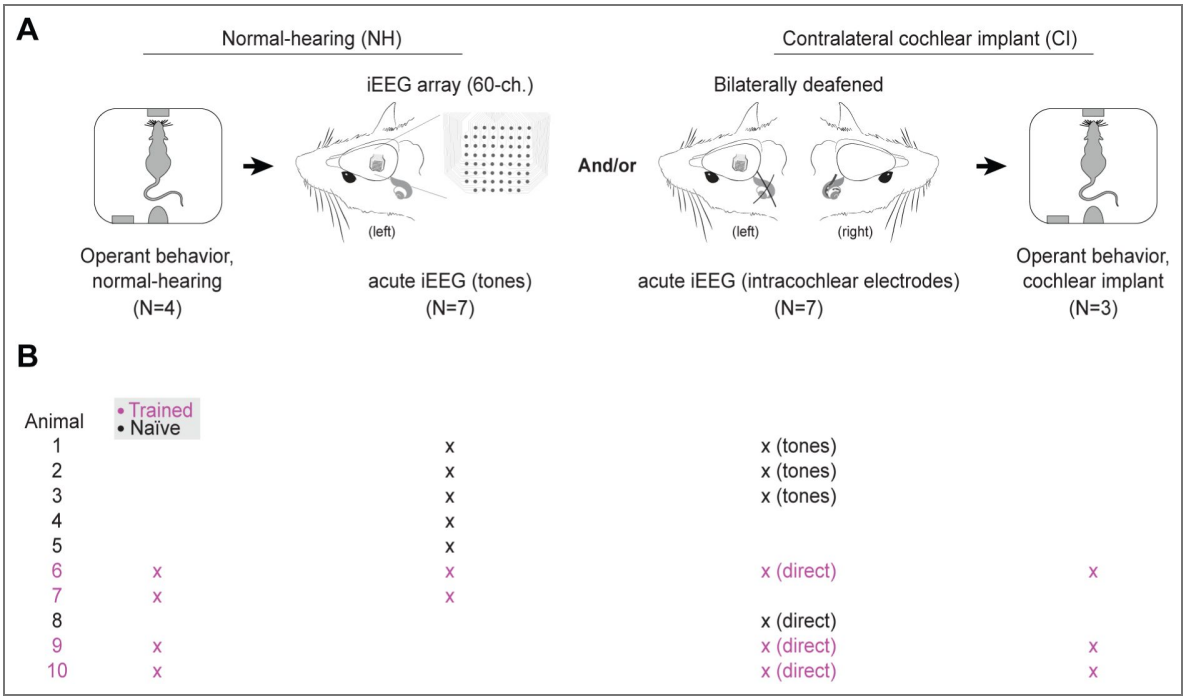

Animal	Trained	Naïve			
1			x	x (tones)	
2			x	x (tones)	
3			x	x (tones)	
4			x		
5			x		
6	x		x	x (direct)	x
7	x		x		
8				x (direct)	
9	x			x (direct)	x
10	x			x (direct)	x

Supplemental Figure 2. Experimental timeline and animal tracker.

A, Rats underwent a combination of behavioral training (when typically-hearing), iEEG recordings, and then behavioral testing (after deafening) in a specific sequence, but not all animals included here participated in every phase. **B,** iEEG measurements were obtained in a total of N=10 animals. In a subset of these animals (N=4), we also obtained iEEG measurements in response to both acoustic tones before deafening and cochlear implant stimulation after deafening. In addition to iEEG recordings, we also behaviorally trained either prior (tones) or after iEEG recordings with cochlear implant stimuli.

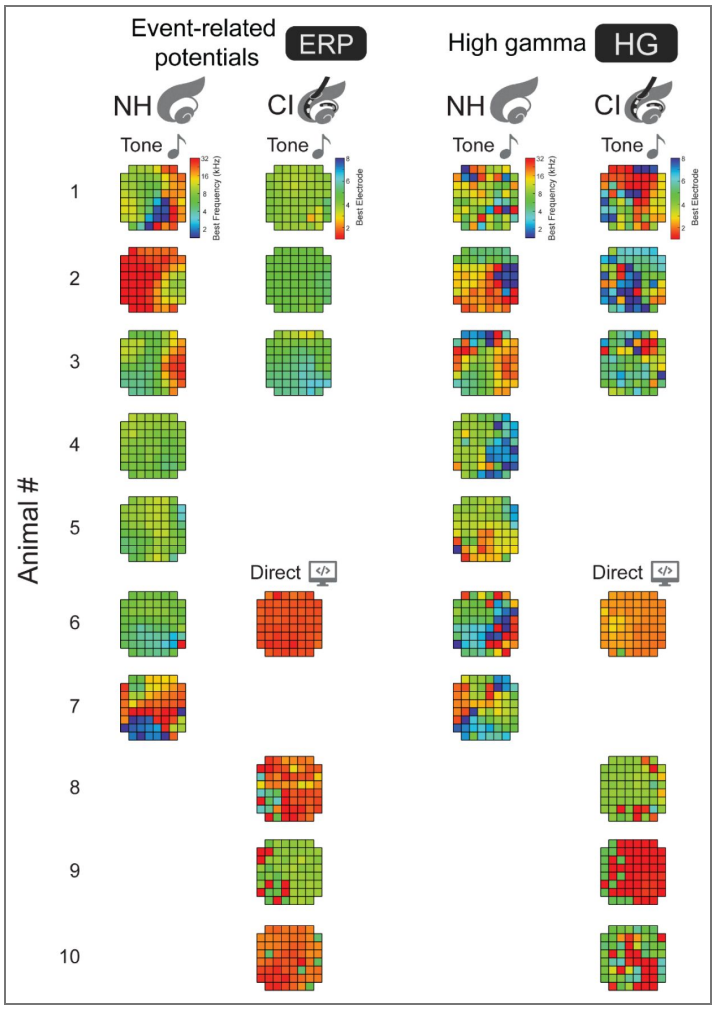

Supplemental Figure 3. Maps of stimulus preferences for tone– or cochlear implant-evoked iEEG measurements.

A, Maps of preferred stimuli are derived from event-related potentials (ERP) for 10 animals, including tone evoked iEEG measurements (left column) and cochlear implant-evoked iEEG measurements (right column). For the cochlear implant, single channel stimuli were either delivered via tones presented to the cochlear implant processor (top 3 maps) and or single channel stimuli were triggered by a direct connection between computer and the cochlear implant processor (bottom 3 maps).

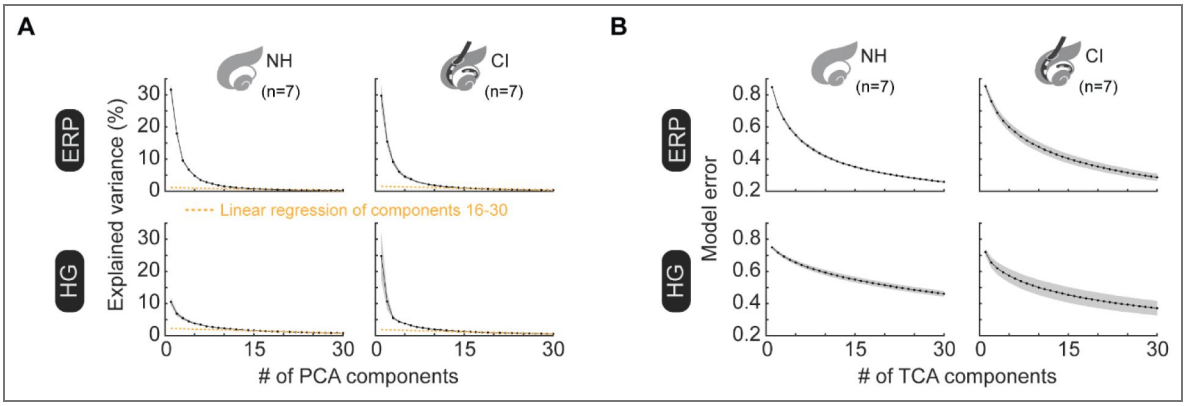

Supplemental Figure 4. Numbers of components for PCA and TCA models

A. The means (±s.e.m.) of explained variance per component for PCA models across all ERP data (top row) decreases rapidly from 30 percent to near zero within 30 components. The means (±s.e.m.) of explained variance per component for PCA models for HG data (bottom row) and decreases from 12 percent rapidly to a steady decline within 30 components. Orange dashed line: linear regression of components 16-30 are plotted. **B.** The means (±s.e.m.) of model error for TCA models of ERP (top row) and HG (bottom row) decrease as a function of number of components.

Data availability

All data and statistics contributing to figures have been deposited at *https://zenodo.org/records/19636556* and are publicly available. The code for essential analyses presented in this paper are accessible at *https://github.com/ahight12/Hight_et_al_2026_eLife* and are publicly available.

Acknowledgements

We thank Badr Albanna, Elad Sagi, and Sam Zheng for comments, discussions, and technical assistance. This work was funded by the National Institute on Deafness and Other Communication Disorders (K99DC021727 to A.E.H., DC015543 to M.N.I., F30DC015170 to J.K.S., and R01DC012557 to R.C.F. and M.A.S.), the National Center for Advancing Translational Sciences (TL1TR001447 to A.E.H.), and the Charles H. Revson Foundation (to A.E.H.); the statements made and views expressed, however, are solely the responsibility of its authors. The current affiliation for Julia K. Scarpa is Weill Cornell Medicine, New York, NY 10065; for Yew-Song Cheng is Massachusetts Eye and Ear Infirmary, Harvard Medical School, Boston MA, 02114; for Michael Trumpis is Paradromics Inc., Austin TX 78759.

Additional information

Funding

Funder	Grant reference number	Author
HHS | NIH | National Institute on Deafness and Other Communication Disorders (NIDCD)	K99DC021727	Ariel E Hight
HHS | NIH | National Institute on Deafness and Other Communication Disorders (NIDCD)	F30DC015170	Julia King Scarpa
HHS | NIH | National Institute on Deafness and Other Communication Disorders (NIDCD)	R01DC012557	Robert C Froemke Mario Svirsky
HHS | NIH | National Center for Advancing Translational Sciences (NCATS)	TL1TR001447	Ariel E Hight
Charles H. Revson Foundation (CHRF)		Ariel E Hight
HHS | NIH | National Institute on Deafness and Other Communication Disorders (NIDCD)	DC015543	Michele N Insanally
Brain and Behavior Research Foundation (BBRF)		Michele N Insanally

Author ORCID iDs

Robert C Froemke: https://orcid.org/0000-0002-1230-6811

References

1. **Abdi-Sargezeh B,** Oswal A, Sanei S (2023) Mapping scalp to intracranial EEG using generative adversarial networks for automatically detecting interictal epileptiform discharges. In: 2023 IEEE Statistical Signal Processing Workshop (SSP). pp. 710-714 https://doi.org/10.1109/ssp53291.2023.10207965 | PubMed

2. **Adenis V,** et al. (2024) Asymmetric Pulses Delivered by a Cochlear Implant Allow a Reduction in Evoked Firing Rate and in Spatial Activation in the Guinea Pig Auditory Cortex. *Hearing Research* **447**:109027 https://doi.org/10.1016/j.heares.2024.109027 | PubMed

3. **Ayton LN,** Barnes N, Dagnelie G, Fujikado T, Goetz G, Hornig R, Jones BW, Muqit MMK, Rathbun DL, Stingl K, *et al.* (2020) An update on retinal prostheses. *Clin Neurophysiol* **131**:1383-1398 https://doi.org/10.1016/j.clinph.2019.11.029 | PubMed
4. **Azadpour M,** McKay CM (2012) A psychophysical method for measuring spatial resolution in cochlear implants. *J Assoc Res Otolaryngol* **13**:145-157 https://doi.org/10.1007/s10162-011-0294-z | PubMed
5. **Bader BW,** Kolda TG (2023) Tensor Toolbox for MATLAB. 3.6 Edition.
6. **Beynon AJ,** Luijten BM, Mylanus EAM (2021) Intracorporeal cortical telemetry as a step to automatic closed-loop EEG-based CI fitting: A proof of concept. *Audiol Res* **11**:691-705 https://doi.org/10.3390/audiolres11040062 | PubMed
7. **Bierer JA,** Middlebrooks JC (2002) Auditory cortical images of cochlear-implant stimuli: dependence on electrode configuration. *J Neurophysiol* **87**:478-492 https://doi.org/10.1152/jn.00212.2001 | PubMed
8. **Bierer JA,** Middlebrooks JC (2004) Cortical responses to cochlear implant stimulation: channel interactions. *J Assoc Res Otolaryngol* **5**:32-48 https://doi.org/10.1007/s10162-003-3057-7 | PubMed
9. **Blamey P,** et al. (2013) Factors affecting auditory performance of postlinguistically deaf adults using cochlear implants: an update with 2251 patients. *Audiol Neurootol* **18**:36-47 https://doi.org/10.1159/000343189 | PubMed
10. **Carcea I,** Insanally MN, Froemke RC (2017) Dynamics of auditory cortical activity during behavioural engagement and auditory perception. *Nat Commun* **8**:14412 https://doi.org/10.1038/ncomms14412 | PubMed
11. **Caswell-Midwinter B,** Doney EM, Arjmandi MK, Jahn KN, Herrmann BS, Arenberg JG (2022) The relationship between impedance, programming and word recognition in a large clinical dataset of cochlear implant recipients. *Trends Hear* **26**:23312165211060983 https://doi.org/10.1177/23312165211060983 | PubMed
12. **Chang EF** (2015) Towards large-scale, human-based, mesoscopic neurotechnologies. *Neuron* **86**:68-78 https://doi.org/10.1016/j.neuron.2015.03.037 | PubMed
13. **Clark GM** (2006) The multiple-channel cochlear implant: the interface between sound and the central nervous system for hearing, speech, and language in deaf people-a personal perspective. *Philos Trans R Soc Lond B Biol Sci* **361**:791-810 https://doi.org/10.1098/rstb.2005.1782 | PubMed
14. **Clark GM** (2015) The multi-channel cochlear implant: Multi-disciplinary development of electrical stimulation of the cochlea and the resulting clinical benefit. *Hear Res* **322**:4-13 https://doi.org/10.1016/j.heares.2014.08.002 | PubMed
15. **Cusumano C,** Friedmann DR, Fang Y, Wang B, Roland JT, Waltzman SB (2017) Performance plateau in prelingually and postlingually deafened adult cochlear implant recipients. *Otol Neurotol* **38**:334-338 https://doi.org/10.1097/mao.0000000000001322 | PubMed
16. **Dawson J,** Pierce D, Dixit A, Kimberley TJ, Robertson M, Tarver B, Hilmi O, McLean J, Forbes K, Kilgard MP, *et al.* (2016) Safety, feasibility, and efficacy of vagus nerve stimulation paired with upper-limb rehabilitation after ischemic stroke. *Stroke* **47**:143-150 https://doi.org/10.1161/strokeaha.115.010477 | PubMed
17. **Djourno A,** Eyries C (1957) [Auditory prosthesis by means of a distant electrical stimulation of the sensory nerve with the use of an indwelt coiling]. *Presse Med* **65**:1417 PubMed
18. **Eddington DK,** Dobelle WH, Brackmann DE, Mladejovsky MG, Parkin JL (1978) Auditory prostheses research with multiple channel intracochlear stimulation in man. *Ann Otol Rhinol Laryngol* **87**:1-39 https://doi.org/10.1177/00034894780870s602 | PubMed
19. **Fallon JB,** Shepherd RK, Irvine DRF (2014) Effects of chronic cochlear electrical stimulation after an extended period of profound deafness on primary auditory cortex organization in cats. *Eur J Neurosci* **39**:811-820 https://doi.org/10.1111/ejn.12445 | PubMed

20. **Froemke RC,** Carcea I, Barker AJ, Yuan K, Seybold BA, Martins ARO, Zaika N, Bernstein H, Wachs M, Levis PA, *et al.* (2013) Long-term modification of cortical synapses improves sensory perception. *Nat Neurosci* **16**:79-88 https://doi.org/10.1038/nn.3274 | PubMed

21. **Fukushima M,** Chao ZC, Fujii N (2015) Studying brain functions with mesoscopic measurements: Advances in electrocorticography for non-human primates. *Curr Opin Neurobiol* **32**:124-131 https://doi.org/10.1016/j.conb.2015.03.015 | PubMed

22. **Glennon E,** Svirsky MA, Froemke RC (2020) Auditory cortical plasticity in cochlear implant users. *Curr Opin Neurobiol* **60**:108-114 https://doi.org/10.1016/j.conb.2019.11.003 | PubMed

23. **Glennon E,** Valtcheva S, Zhu A, Wadghiri YZ, Svirsky MA, Froemke RC (2023) Locus coeruleus activity improves cochlear implant performance. *Nature* **613**:317-323 https://doi.org/10.1038/s41586-022-05554-8 | PubMed

24. **Glennon E,** Carcea I, Martins ARO, Multani J, Shehu I, Svirsky MA, Froemke RC (2019) Locus coeruleus activation accelerates perceptual learning. *Brain Res* **1709**:39-49 https://doi.org/10.1016/j.brainres.2018.05.048 | PubMed

25. **Hays SA,** Rennaker RL, Kilgard MP (2013) Targeting plasticity with vagus nerve stimulation to treat neurological disease. *Prog Brain Res* **207**:275-299 https://doi.org/10.1016/b978-0-444-63327-9.00010-2 | PubMed

26. **Hochmair ES,** Hochmair-Desoyer IJ (1981) An implanted auditory eight channel stimulator for the deaf. *Med Biol Eng Comput* **19**:141-148 https://doi.org/10.1007/bf02442707 | PubMed

27. **Hochmair I,** et al. (2006) MED-EL cochlear implants: State of the art and a glimpse into the future. *Trends Amplif* **10**:201-219 https://doi.org/10.1177/1084713806296720 | PubMed

28. **Holden LK,** Finley CC, Firszt JB, Holden TA, Brenner C, Potts LG, Gotter BD, Vanderhoof SS, Mispagel K, Heydebrand G, *et al.* (2013) Factors affecting open-set word recognition in adults with cochlear implants. *Ear Hear* **34**:342-360 https://doi.org/10.1097/aud.0b013e3182741aa7 | PubMed

29. **House WF,** Urban J (1973) Long term results of electrode implantation and electronic stimulation of the cochlea in man. *Ann Otol Rhinol Laryngol* **82**:504-517 https://doi.org/10.1177/000348947308200408 | PubMed

30. **Insanally M,** Trumpis M, Wang C, Chiang C-H, Woods V, Palopoli-Trojani K, Bossi S, Froemke RC, Viventi J (2016) A low-cost, multiplexedμECoG system for high-density recordings in freely moving rodents. *J Neural Eng* **13**:026030-26030 https://doi.org/10.1088/1741-2560/13/2/026030 | PubMed

31. **Insanally MN,** Albanna BF, Toth J, DePasquale B, Fadaei SS, Gupta T, Lombardi O, Kuchibhotla K, Rajan K, Froemke RC (2024) Contributions of cortical neuron firing patterns, synaptic connectivity, and plasticity to task performance. *Nat Commun* **15**:6023 https://doi.org/10.1038/s41467-024-49895-6 | PubMed

32. **Janiukstyte V,** Owen TW, Chaudhary UJ, Diehl B, Lemieux L, Duncan JS, de Tisi J, Wang Y, Taylor PN (2023) Normative brain mapping using scalp EEG and potential clinical application. *Sci Rep* **13**:13442 https://doi.org/10.1038/s41598-023-39700-7 | PubMed

33. **Jasper H,** Penfield W (1949) Electrocorticograms in man: Effect of voluntary movement upon the electrical activity of the precentral gyrus. *Archiv für Psychiatrie und Nervenkrankheiten* **183**:163-174 https://doi.org/10.1007/bf01062488

34. **Johnson KA,** et al. (2024) Proceedings of the 11th Annual Deep Brain Stimulation Think Tank: pushing the forefront of neuromodulation with functional network mapping, biomarkers for adaptive DBS, bioethical dilemmas, AI-guided neuromodulation, and translational advancements. *Front Hum Neurosci* **18**:1320806 https://doi.org/10.3389/fnhum.2024.1320806 | PubMed

35. **Johnson LA,** Della Santina CC, Wang X (2016) Selective neuronal activation by cochlear implant stimulation in auditory cortex of awake primate. *J Neurosci* **36**:12468-12484 https://doi.org/10.1523/jneurosci.1699-16.2016 | PubMed

36. **Keating P,** Nodal FR, Gananandan K, Schulz AL, King AJ (2013) Behavioral sensitivity to broadband binaural localization cues in the ferret. *J Assoc Res Otolaryngol* **14**:561-572 https://doi.org/10.1007/s10162-013-0390-3 | PubMed

37. **King J,** Shehu I, Roland JT, Svirsky MA, Froemke RC (2016) A physiological and behavioral system for hearing restoration with cochlear implants. *J Neurophysiol* **116**:844-858 https://doi.org/10.1152/jn.00048.2016 | PubMed

38. **Klinke R,** Kral A, Heid S, Tillein J, Hartmann R (1999) Recruitment of the auditory cortex in congenitally deaf cats by long-term cochlear electrostimulation. *Science* **285**:1729-1733 https://doi.org/10.1126/science.285.5434.1729 | PubMed

39. **Kolda TG,** Bader BW (2009) Tensor Decompositions and Applications. *SIAM Review* **51**:455-500

40. **Kral A,** et al. (2002) Hearing after congenital deafness: Central auditory plasticity and sensory deprivation. *Cereb Cortex* **12**:797-807 https://doi.org/10.1093/cercor/12.8.797 | PubMed

41. **Kral A,** Eggermont JJ (2007) What's to lose and what's to learn: Development under auditory deprivation, cochlear implants and limits of cortical plasticity. *Brain Res Rev* **56**:259-269 https://doi.org/10.1016/j.brainresrev.2007.07.021 | PubMed

42. **Martins ARO,** Froemke RC (2015) Coordinated forms of noradrenergic plasticity in the locus coeruleus and primary auditory cortex. *Nat Neurosci* **18**:1483-1492 https://doi.org/10.1038/nn.4090 | PubMed

43. **McDermott HJ** (2004) Music perception with cochlear implants: a review. *Trends Amplif* **8**:49-82 https://doi.org/10.1177/108471380400800203 | PubMed

44. **Merzenich MM,** Knight PL, Roth GL (1973) Cochleotopic organization of primary auditory cortex in the cat. *Brain Res* **63**:343-346 https://doi.org/10.1016/0006-8993(73)90101-7 | PubMed

45. **Mesgarani N,** Cheung C, Johnson K, Chang EF (2014) Phonetic feature encoding in human superior temporal gyrus. *Science* **343**:1006-1010 https://doi.org/10.1126/science.1245994 | PubMed

46. **Michelson RP** (1971) The results of electrical stimulation of the cochlea in human sensory deafness. *Ann Otol Rhinol Laryngol* **80**:914-919 https://doi.org/10.1177/000348947108000618 | PubMed

47. **Middlebrooks JC,** Bierer JA (2002) Auditory cortical images of cochlear-implant stimuli: coding of stimulus channel and current level. *J Neurophysiol* **87**:493-507 https://doi.org/10.1152/jn.00211.2001 | PubMed

48. **Moore DR,** Shannon RV (2009) Beyond cochlear implants: awakening the deafened brain. *Nat Neurosci* **12**:686-691 https://doi.org/10.1038/nn.2326 | PubMed

49. **Norman-Haignere SV,** Long LK, Mesgarani N, Devinsky O, Flinker A, Doyle W, Irobunda I, Merricks EM, Schevon CA, Feldstein NA, *et al.* (2022) Multiscale temporal integration organizes hierarchical computation in human auditory cortex. *Nat Hum Behav* **6**:455-469 https://doi.org/10.1038/s41562-021-01261-y | PubMed

50. **Nourski KV,** Etler CP, Brugge JF, Oya H, Kawasaki H, Reale RA, Abbas PJ, Brown CJ, Howard MA (2013) Direct recordings from the auditory cortex in a cochlear implant user. *J Assoc Res Otolaryngol* **14**:435-450 https://doi.org/10.1007/s10162-013-0382-3 | PubMed

51. **Polley DB,** Read HL, Storace DA, Merzenich MM (2007) Multiparametric auditory receptive field organization across five cortical fields in the albino rat. *J Neurophysiol* **97**:3621-3638 https://doi.org/10.1152/jn.01298.2006 | PubMed

52. **Ray S,** Maunsell JH (2011) Different origins of gamma rhythm and high-gamma activity in macaque visual cortex. *PLoS Biol* **9**:e1000610 https://doi.org/10.1371/journal.pbio.1000610 | PubMed

53. **Simmons FB,** Epley JM, Lummis RC, Guttman N, Frishkopf LS, Harmon LD, Zwicker E (1965) Auditory Nerve: Electrical Stimulation in Man. *Science* **148**:104-106 https://doi.org/10.1126/science.148.3666.104 | PubMed

54. **Stronks HC,** Arendsen TS, Veenstra M, Boermans P-PBM, Briaire JJ, Frijns JHM (2025) Effects of preoperative factors on the learning curves of postlingual cochlear implant recipients. *Ear Hear (in press)* https://doi.org/10.1097/aud.0000000000001690 | PubMed

55. **Svirsky M** (2017) Cochlear implants and electronic hearing. *Physics Today* **70**:52-58 https://doi.org/10.1063/pt.3.3661

56. **Tang C,** Hamilton LS, Chang EF (2017) Intonational speech prosody encoding in the human auditory cortex. *Science* **357**:797-801 https://doi.org/10.1126/science.aam8577 | PubMed

57. **Trumpis M,** Insanally M, Zou J, Elsharif A, Ghomashchi A, Sertac Artan N, Froemke RC, Viventi J (2017) A low-cost, scalable, current-sensing digital headstage for high channel count muECoG. *J Neural Eng* **14**:026009 https://doi.org/10.1088/1741-2552/aa5a82 | PubMed

58. **Vermeire K,** Landsberger DM, Schleich P, Van de Heyning PH (2013) Multidimensional scaling between acoustic and electric stimuli in cochlear implant users with contralateral hearing. *Hear Res* **306**:29-36 https://doi.org/10.1016/j.heares.2013.09.004 | PubMed

59. **Vollmer M,** Beitel RE (2011) Behavioral training restores temporal processing in auditory cortex of long-deaf cats. *J Neurophysiol* **106**:2423-2436 https://doi.org/10.1152/jn.00565.2011 | PubMed

60. **Walzl EM,** Woolsey CN (1946) Effects of cochlear lesions on click responses in the auditory cortex of the cat. *Bull Johns Hopkins Hosp* **79**:309-319 PubMed

61. **Williams AH,** Kim TH, Wang F, Vyas S, Ryu SI, Shenoy KV, Schnitzer M, Kolda TG, Ganguli S (2018) Unsupervised Discovery of Demixed, Low-Dimensional Neural Dynamics across Multiple Timescales through Tensor Component Analysis. *Neuron* **98**:1099-1115 https://doi.org/10.1016/j.neuron.2018.05.015 | PubMed

62. **Wilson BS,** Finley CC, Lawson DT, Wolford RD, Eddington DK, Rabinowitz WM (1991) Better speech recognition with cochlear implants. *Nature* **352**:236-238 https://doi.org/10.1038/352236a0 | PubMed

63. **Wilson BS,** Dorman MF (2008) Cochlear implants: A remarkable past and a brilliant future. *Hear Res* **242**:3-21 https://doi.org/10.1016/j.heares.2008.06.005 | PubMed

64. **Woods V,** Trumpis M, Bent B, Palopoli-Trojani K, Chiang C-H, Wang C, Yu C, Insanally MN, Froemke RC, Viventi J (2018) Long-term recording reliability of liquid crystal polymer µECoG arrays. *J Neural Eng* **15**:066024 https://doi.org/10.1088/1741-2552/aae39d | PubMed

65. **Zeng FG** (2022) Celebrating the one millionth cochlear implant. *JASA Express Lett* **2**:077201 https://doi.org/10.1121/10.0012825 | PubMed

Peer reviews

Reviewer #1 (Public review):

Summary

This manuscript addresses an important question in auditory neuroscience and neuroprosthetics: whether cortical responses to cochlear implant stimulation resemble those evoked by natural acoustic stimulation, or whether electrical stimulation engages a distinct cortical representation. The authors use high-density intracranial EEG recordings in rats to compare responses to pure tones in normal-hearing animals with responses to single-channel cochlear implant stimulation in deafened animals. They combine analyses of event-related potentials, high-gamma activity, trial-by-trial variability, PCA/TCA-based dimensionality reduction, and decoder-based measures of stimulus information.

Strengths

A major strength of the study is the question it addresses. Understanding how electrical cochlear stimulation is represented centrally is highly relevant for cochlear implant design, fitting strategies, and rehabilitation. The comparison between acoustic and electrical stimulation, including within-animal comparisons in a subset of cases, is valuable because it directly addresses whether implant-evoked activity can be interpreted within the framework of normal acoustic tonotopy.

The methodological approach is also a strength. Dense cortical surface recordings provide simultaneous access to spatial and temporal features of auditory cortical responses. The combination of PCA, TCA, and decoder analyses gives complementary views of the data, and the information-transfer analysis provides an interesting way to ask whether representations learned from acoustic stimulation generalize to electrical stimulation.

Weaknesses:

The main weakness is that the evidence for spatial organization remains difficult to interpret. In Figure 2, the authors argue that both tone-evoked and cochlear implant-evoked responses are spatially organized, but the slope analyses are not significant for the cochlear implant condition. The revised vector-strength analysis supports the presence of non-random spatial structure, but this is not the same as demonstrating a clear graded cochleotopic organization. The manuscript would be strongest if it consistently distinguished between non-random spatial structure, coarse topography, and true graded tonotopy or cochleotopy.

A related issue is that some figure titles and interpretive statements still appear stronger than the data justify. For example, the TCA results in Figure 7 are described as revealing topographically organized latent spatial factors, but the statistical support appears strongest for normal-hearing high-gamma responses, with weaker or non-significant results in other conditions. These data remain interesting, but they would be better framed as evidence for weak or coarse spatial structure rather than robust topographic organization across all modalities.

The decoder analyses are improved, especially with the added tone-to-tone control. This control supports the conclusion that poor acoustic-to-CI transfer is not simply a failure of the TCA/LDA pipeline. However, the analysis remains model-dependent, and the absolute information transfer values are low. It would be helpful either to include an analogous analysis using raw ERP/high-gamma features or to explain more explicitly why the TCA-based approach is the appropriate primary test. The data support poor generalization between acoustic and implant-evoked cortical responses, but claims about perceptual qualities should remain speculative because perception is not directly measured in these experiments.

Finally, although methodological reporting is much improved, some verification remains indirect. The authors provide useful implantation criteria and cite prior validation of their deafening approach, but the manuscript would be clearer if it explicitly distinguished between validation performed in the present animals and validation based on previous cohorts. This distinction is important because surgical variability, implantation efficacy, and deafening completeness can influence the interpretation of cochlear implant experiments.

Comments on revised version.

The revised manuscript is considerably improved. The authors have clarified several methodological details, added a statistical framework that better accommodates both paired and unpaired animals, provided a clearer account of animal cohorts, added peripheral ECAP/forward-masking data to support the cochlear specificity of implant stimulation, and included a useful positive control for the cross-modal decoder analysis. These additions make the manuscript stronger and help readers interpret the main findings more confidently.

The results support the conclusion that acoustic and cochlear implant stimulation evoke cortical responses with different properties. In particular, acoustic responses support better single-trial stimulus decoding than cochlear implant responses, and decoders trained on acoustic responses transfer poorly to implant-evoked responses. The evidence for spatial organization is more nuanced. The cochlear implant condition shows evidence of non-random spatial structure, but not a clear graded cochleotopic map. The normal-hearing condition is also less visually clear than might be expected from prior tonotopy studies,

although the added analyses and comparisons to previous work help contextualize this result. Overall, the study makes a valuable contribution, provided that the claims about spatial organization and perceptual interpretation remain appropriately cautious.

The revision addresses several important concerns from the original version. The use of mixed-effects models better matches the partially paired experimental design. The expanded Methods improve reproducibility. The new cohort schematic helps clarify which animals contributed to behavioral and neural datasets. The ECAP forward-masking measurements add useful peripheral validation, and the within-modality decoder control strengthens the interpretation of the poor cross-modal transfer result. Together, these changes substantially improve the manuscript.

The work is likely to be of interest to auditory neuroscientists, cochlear implant researchers, and neuroengineers. Even where some conclusions require cautious wording, the dataset and analytical framework may be useful for future studies aiming to relate cortical responses to implant programming, perceptual learning, or closed-loop neuroprosthetic approaches.

Overall, the revised manuscript is stronger and addresses an important problem with useful methods and analyses. The results most convincingly show that acoustic responses support better single-trial decoding than acute cochlear implant responses, and that acoustic-trained decoders generalize poorly to implant-evoked activity. The evidence for robust spatial organization, especially in the cochlear implant condition, is more limited and should be presented with appropriate caution.

https://doi.org/10.7554/eLife.108550.2.sa3

Reviewer #2 (Public review):

Summary:

This article reports measurements of iEEG signals on the rat auditory cortex during cochlear implant or sound stimulation in separate groups of rats. The observations indicate some spatial organization of cochlear implant stimuli, but that is very different from cochlear implants.

Strengths:

The study includes interesting analyses of the sound and cochlear implant representation structure based on decoders.

Weaknesses:

The observation that responses to cochlear implant stimulation (stimulation) is spatially organized is not new (e.g. Adenis et al. 2024)

The claim that spatial and temporal dimensions contribute information about the sound is also not new there is a large literature on this topic.

The analyses supporting the claim that there is a mismatch between cochlear implant and sound representation are still unclear, particularly in Fig. 8.

https://doi.org/10.7554/eLife.108550.2.sa2

Reviewer #3 (Public review):

Summary:

Through micro-electroencephalography, Hight and colleagues studied how the auditory cortex in its ensemble respond to cochlear implant stimulation compared to the classic pure tones. Taking advantage of a double implanted rat model (Micro-ECoG and Cochlear Implant), they tracked and analyzed changes happening in the temporal and spatial aspects of the cortical evoked responses in both normal hearing and cochlear-implanted animals. After establishing that single trial responses were sufficient to encode the stimuli properties, the authors then explored several decoder architectures to study the cortex ability to encode each stimuli modality in a similar or different manner. They conclude that a) intracranial EEG evoked responses can be accurately recorded and did not differed between normal hearing and cochlear-implanted rats; b) Although coarsely spatially organized, CI-evoked responses had higher trial-by-trial variability than pure tones; c) Stimulus identity is independently represented by temporal and spatial aspect of cortical representations and can be accurately decoded by various means from single trials; d) and that Pure tones trained decoder can't decode CI-stimulus identity accurately.

Strength:

The model combining micro-eCoG and cochlear implantation and the methodology to extract both the Event Related Potentials (ERPs) and High-Gammas (HGs) is very well designed and appropriately analyzed. Likewise, the PCA-LDA and TCA-LDA are powerful tools that take full advantage of the information provided by the cortical ensembles.

The overall structure of the paper, with a paced and exhaustive progress through each step and evolution of the decoder is very appreciable and easy to follow. The exploration of single trial encoding and stimulus identity through temporal and spatial domains is providing new avenues to characterize the cortical responses CI stimulations and their central representation. The fact that single trials suffice to decode the stimulus identity regardless of their modality is of great interest and noteworthy. Although the authors confirm that iEEG remains difficult to transpose in clinic, the insights provided by the study confirm the potential benefit of using central decoders to help in clinic settings.

Weakness:

The conclusion of the paper, especially the concept of distinct cortical encoding for each modality, is unfortunately partially supported by the results as the authors ignored fundamental limitations of CI related stimulation.

First, the authors stimulated in a Monopolar mode which, albeit being clinically relevant, notoriously generates a high current spread in rodent models. Comparing the averaged BF maps for iEEG (Fig-2A, C), BFs ranged from 4 to 16kHz with a predominance of 4kHz BFs. The lack of BFs at higher frequencies might reveal a potential location mismatch between the frequency range sampled at the level of the cortex (low to medium frequencies) and the frequency range covered by the CI inserted mostly in the first turn-and-a-half of the cochlea (high to medium frequencies). Looking at Fig-2F (and to some extend 2A) most of CI electrodes elicited responses around the 4kHz regions and averaged maps show a predominance of CI-3-4 across cortex (Fig-2C, H and Sup Fig. 3) from areas with 4kHz BF to areas with 16kHz BF. It is doubtful that CI-3-4 are located near the 4kHz region based on Müller's work (1991) on the frequency representation in the rat cochlea. Moreover, Supplemental figure 3 shows that only a couple of CI electrodes are predominately represented at the level of the cortex. Thus, it seems possible that current spread ended stimulating indistinctly higher turns of the cochlea or even the modiolus in a non-specific manner, greatly reducing (or smearing) the place-coding/frequency resolution of each electrode, which in turn could explain the coarse topographic (or coarsely tonotopic according to the manuscript) organization of the cortical responses.

Second, although the authors acknowledge that post-lingual CI users always have an adaptation period, their conclusion is based on measurements that are relatively "early" in the CI-use timeline so to speak since iEEG were collected a) acutely right after mono-aural implantation and stimulation, b) under anesthesia, c) using unmodulated pulse train fixed at 900pps regardless of the electrode used and thus lacking any temporal information shifts in relationship to electrode cochleotopic placement. Basically, all CI electrodes had the same rate whereas you would expect basal CI electrodes to be amplitude modulated at higher frequencies than apical electrodes.

As much as the reviewer likes the overall approach with the use of PCA-LDA and TCA, and agrees that information transfer seems inexistant at time of measurement, authors should be more careful in their strong conclusion that two distinct encoding exist. The non-overlapping between sound and electric stimulation representations might exist only transiently and this should be acknowledged a bit more in the discussion. Without repetition of iEEG measurement at later period with chronic use of the CI, it is not possible to definitively claim that two distinct, non-overlapping coding co-exist at all times.

Nevertheless, the reviewer wants to reiterate that the study proposed by Hight et al. is well constructed, relevant to the field and that the overall proposal of improving patient performances and help their adaptation in the first months of CI use by studying central responses should be pursued as it might help establish new guidelines or create new clinical tools.

https://doi.org/10.7554/eLife.108550.2.sa1

Author response:

The following is the authors' response to the original reviews

Summary of revision for all referees:

We thank referees for their constructive comments. To address their concerns, we now performed additional statistical analyses integrating both paired and unpaired data, performed positive controls for comparisons between NH- and CI- evoked iEEG measurements, developed tools for measuring and collected new experimental data on forward masking ECAP measurements in CI implanted rats (N=3), and reworked both manuscript text and figures to improve clarity. These most significant changes are summarized here, and a complete list of responses to reviewers and corresponding changes will follow.

Summary of major changes to revised manuscript:

(1) Statistical treatment of paired vs unpaired recordings using mixed-effects models (updates to all manuscript figures that compare NH vs CI); this largely confirmed the results reported in our original submission.

(2) New analysis, controlling for information-theoretic cross-modality comparison (i.e., training with tone- and testing with cochlear implant-evoked iEEG measures, Fig. 8).

(3) Clarification of methods (Supplemental Fig. 2 & manuscript text)

(4) Additional experiments testing peripheral tuning of our 8-channel CI rodent model via forward masking ECAP measures across 3 animals (N=3, Supplemental Fig. 1)

(5) Detailed response addressing robustness of tonotopy in NH and CI animals

> ***Public Reviews:***

> ***Reviewer #1 (Public Review):***
>
> *Strengths:*
>
> *The study poses a timely, clinically relevant question with clear implications for CI strategy. The analytical toolkit is appropriate: µECoG captures mesoscale patterns; TCA offers a transparent separation of spatial and temporal structure; and mutual-information decoding provides an interpretable measure of single-trial discriminability. Within-subject recordings in a subset of animals, in principle, help isolate modality effects from inter-animal variability. Where analyses are most direct, the acoustic condition yields higher single-trial decoding accuracy, which is a meaningful and clearly presented result.*

We appreciate the comments on the strengths of our analytic approaches.

> *Weaknesses:*
>
> *Parts of the statistical treatment do not match the data structure: some comparisons mix paired and unpaired animals but are analysed as fully paired, raising concerns about misestimated uncertainty.*

Please see our response to specific comment #2 above. In short, we agree with this critique of our original analyses, and in our revised manuscript we re-analyzed all NH vs. CI comparisons using linear mixed effects models that incorporate both paired and unpaired observations within a single framework. This allows us to include all animals, account for within-animal dependence for paired experiments (normal hearing and cochlear implant data from the same animal when available), and to align the statistical tests with the data shown in the figures. In almost every case, the mixed effects models confirm our original conclusions. Two comparisons that were previously nonsignificant now reach criterion for statistical significance (Fig. 2E, p=0.048 and Fig. 6F, p=0.027). We updated the manuscript to report these values and to clarify the use of mixed effects modeling in the methods under the section titled, “Linear mixed effects modeling.”

> *Methodological reporting is incomplete in places; essential parameters for both acoustic and electrical stimulation, as well as objective verification of implantation and deafening, are not described with sufficient detail to support confident interpretation or replication.*

Please see our response to comment #5 below. We have revised our manuscript to now include this information in the methods.

> *Figure-level clarity also undermines the message. In Figure 2, non-significant slopes for CI, repeated identification of a single "best channel," mismatched axes, and unclear distinctions between example and averaged panels make the assertion of spatial organisation unconvincing; importantly, the normal-hearing panels also do not display tonotopy as clearly as expected, which weakens the key contrast the paper seeks to establish.*

This is an important point, thanks- please see responses to comment #1 above. We note that conventional tonotopic maps in auditory cortex are characteristic frequency maps, i.e., maps of topographic organization for responses to lowest-threshold stimuli (often presented around 20-50 dB SPL). Our maps were constructed from stimuli presented at 70 dB SPL, thus blunting crisp tonotopy to some degree. Furthermore, we quantified spatial organization using a previously published method from the Polley lab (Romero & Hight et al. 2020), in which local tonotopic gradient vectors (magnitude and direction) were computed from GCaMP responses at each pixel and projected onto a unit circle. Mean vector strength across all pixels was then compared to a shuffled distribution as a measure of tonotopic

organization. We applied the same procedure to our iEEG best-frequency and best-channel maps. Both map types yielded mean vector strengths that were substantially larger than those derived from shuffled maps ($p < 10^{-10}$), indicating that our maps have a consistent tonotopic (for BFs) or cochleotopic (for CI channels) organization that is highly unlikely to arise by chance. This is now included in our revised manuscript.

> *Finally, the decoding claims would be strengthened by simple internal controls, such as within modality train/test splits and decoding on raw ERP/high-gamma features to demonstrate that poor cross-modal transfer reflects genuine differences in the underlying responses rather than limitations of the modelling pipeline.*

Please see our response to comment #12 below. In short, we have now included this analysis in revised Figure 8.

> ***Reviewer #2 (Public Review):***
>
> *Strengths:*
>
> *The study includes interesting analyses of the sound and cochlear implant representation structure based on decoders.*

We appreciate the comment on how interesting our analyses are, thanks!

> *Weaknesses:*
>
> *The observation that responses to cochlear implant stimulation (stimulation) are spatially organized is not new (e.g., Adenis et al. 2024).*

We agree that it is not particularly novel to report that there is spatial organization to cochlear implant stimulation. However, we believe that our direct comparisons (when possible, within animal) between normal-hearing and cochlear implant modality maps is unusual in the literature, including asking how decoders based on one set of responses might apply to responses evoked from the other modality. Adenis et al. (2024) is a fantastic study of pulse shape and monopolar vs bipolar stimulation modes with a 6-channel implant in guinea pig, but as far as we can tell this study does also not compare normal hearing maps prior to deafening and implantation to the cochlear implant maps in the same animals.

> *The claim that spatial and temporal dimensions contribute information about the sound is also not new; there is a large literature on this topic. Moreover, the results shown here are extremely weak. They show similar levels of information in the spatial and temporal dimensions, and no synergy between the two dimensions. This is however, likely the consequence of high measurement noise leading to poor accuracy in the information estimates, as the authors state.*

Good point, please see our response to comment #1 below.

> *The main claim of the study - the mismatch between cochlear implant and sound representation - is not supported. The responses to each modality are measured in different animals. The authors do not show that they actually can compare representations across animals (e.g., for the same sounds). Without this positive control, there is no reason to think that it is possible to decode from one animal with a decoder trained on another, and the negative result shown by the authors is therefore not surprising.*

Good point, thanks- please see our response to comment #2 below, where we describe this new control we have added.

> ***Reviewer #3 (Public Review):***

> *Strengths:*
>
> *The model combining micro-eCoG and cochlear implantation and the methodology to extract both the Event Related Potentials (ERPs) and High-Gammas (HGs) is very well designed and appropriately analyzed. Likewise, the PCA-LDA and TCA-LDA are powerful tools that take full advantage of the information provided by the cortical ensembles. The overall structure of the paper, with a paced and exhaustive progress through each step and evolution of the decoder, is very appreciable and easy to follow. The exploration of single-trial encoding and stimulus identity through temporal and spatial domains is providing new avenues to characterize the cortical responses to CI stimulations and their central representation. The fact that single trials suffice to decode the stimulus identity regardless of their modality is of great interest and noteworthy. Although the authors confirm that iEEG remains difficult to transpose in the clinic, the insights provided by the study confirm the potential benefit of using central decoders to help in clinic settings… the reviewer wants to reiterate that the study proposed by Hight et al. is well constructed, relevant to the field, and that the overall proposal of improving patient performances and helping their adaptation in the first months of CI use by studying central responses should be pursued as it might help establish new guidelines or create new clinical tools.*

We thank the Reviewer for the positive comments about the thoroughness of our analyses and clear organization of our manuscript.

> *Weaknesses:*
>
> *The conclusion of the paper, especially the concept of distinct cortical encoding for each modality, is unfortunately partially supported by the results, as the authors did not adequately consider fundamental limitations of CI-related stimulation. First, the reviewer assumed that the authors stimulated in a Monopolar mode, which, albeit being clinically relevant, notoriously generates a high current spread in rodent models.*

Thanks, this is an important potential concern. Please see our response to comment #5 of Referee 1 and responses to comment #3 below. We agree that monopolar stimulation would be expected to be less spatially specific than bipolar or multipolar modes. However, we chose monopolar stimulation because it is the main clinical configuration in human CI users and therefore most relevant for translational purposes. For our revised manuscript, we made new ECAP measurements of peripheral (spatial and temporal) tuning via a forward masking paradigm and demonstrate that monopolar is effectively tuned (Supplemental Fig. 2). Together with additional single-animal maps in Supplementary Figure 3, together with our vector-strength analysis (Response Fig. 2), demonstrate that even under acute monopolar stimulation we observe structured cochleotopic organization in cortex, rather than the extremely low-pass patterns one might expect if monopolar spread was a major contaminant.

> *Second, comparing the averaged BF maps for iEEG (Figure 2A, C), BFs ranged from 4 to 16kHz with a predominance of 4kHz BFs. The lack of BFs at higher frequencies hints at a potential location mismatch between the frequency range sampled at the level of the cortex (low to medium frequencies) and the frequency range covered by the CI inserted mostly in the first turn-and-a-half of the cochlea (high to medium frequencies). Looking at Figure 2F (and to some extent 2A), most of the CI electrodes elicited responses around the 4kHz regions, and averaged maps show a predominance of CI-3-4 across the cortex (Figure 2C, H) from areas with 4kHz BF to areas with 16kHz BF. It is doubtful that CI-3-4 are located near the 4kHz region based on Müller's work (1991) on the frequency representation in the rat cochlea.*

Please see our responses to comment #3 below.

> *Taken together with the Pearsons correlations being flat, the decoder examples showing a strong ability to identify CI-4 and 3 and the Fig-8D, E presenting a strong prediction of 4kHz and 8kHz for all the CI electrodes when using a pure tone trained decoder, it is possible that current spread ended stimulating indistinctly higher turns of the cochlea or even the modiolus in a non-specific manner, greatly reducing (or smearing) the place-coding/frequency resolution of each electrode, which in turn could explain the coarse topographic (or coarsely tonotopic according to the manuscript) organization of the cortical responses. Thus, the conclusion that there are distinct encodings for each modality is biased, as it might not account for monopolar smearing. To that end, and since it is the study's main message and title, it would have benefited from having a subgroup of animals using bipolar stimulations (or any focused strategy since they provide reduced current spread) to compare the spatial organization of iEEG responses and the performances of the different decoders to dismiss current spread and strengthen their conclusion.*

Please see our responses to comment #4 below as well as our responses related to monopolar vs bipolar stimulation. We agree that for future studies, it will be important to do a heads-on comparison of the differences between bipolar and monopolar stimulation depending on electrode location and stimulation intensity.

> ***Recommendations for the authors:***
>
> ***Reviewer #1 (Recommendations for the authors):***

We thank the reviewer for commenting on the strengths of our manuscript, including appreciating the power and timeliness of our approach.

> *(1a) Figure 2 does not convincingly support the claim that "tone-evoked and CI-evoked iEEG measurements are spatially organized," particularly for CI data: Figure 2C repeatedly highlights the same "best channel," and the slopes in Figures 2B and 2G are non-significant; there are also discrepancies between panels (A vs. C, F vs. H) and mismatched frequency ranges (0-16 kHz vs. up to 32 kHz), which should be clarified as exemplar versus averaged displays and harmonized in scale.*

(First we note that Reviewer 3 also raised related concerns about the robustness of tonotopy in our iEEG data.) We address these by comparing our maps to previously published tonotopic maps, and using an established quantitative analysis of tonotopic strength from Romero & Hight et al. (2020).

First, to place our tone-evoked iEEG maps in context, we overlaid them on the same spatial scale and orientation as both single-unit tonotopy in rat primary auditory cortex (A1) from Polley et al. (2006) and iEEG maps obtained with the same surface array in Insanally et al. (2016). The rostral–caudal and dorsal–ventral axes and cortical extents are matched across panels. Our best-frequency maps (Figure 2C) qualitatively recapitulate the high-to-low frequency gradient and spatial layout reported in both of these prior studies, supporting our claim that tone-evoked iEEG captures canonical mesoscale tonotopy. We have updated the manuscript results section to directly reference these two studies, “The area and orientations of tone-evoked maps qualitatively match those published from single unit recordings (Polley et al. 2006) and published using similar iEEG arrays (Insanally et al. 2016).”

Second, to quantify tonotopy in a way that is directly comparable to previous work, we reproduced the analysis of Romero & Hight et al. (2020), who examined tone-evoked GCaMP signals (Romero & Hight et al. (2020)). In that paper, local tonotopic gradient vectors (magnitude and direction) were computed at each pixel and projected onto a unit circle; the mean vector strength across all pixels was then compared to a shuffled distribution as a measure of tonotopic organization. We applied the same procedure to our iEEG best-

frequency and best-channel maps (Fig. 2C-E). Both map types yielded mean vector strengths that were substantially larger than those derived from shuffled maps ($p < 10^{-10}$), indicating that our maps have a consistent tonotopic (for BFs) or cochleotopic (for CI channels) organization that is highly unlikely to arise by chance. We cite this paper for these analyses related to Figure 2.

> *(1b) Figure 2C repeatedly highlights the same 'best channel'*

We agree that many CI-evoked maps are dominated by a single channel, as seen in our exemplar and in the additional animals shown in new Supplemental Fig. 3. In Fig. 2C, channel 5 emerges as the dominant best channel, as CI-evoked activity in this animal is broad and is strongest for channel 5 (Fig. 2A). This reflects a feature of iEEG signals rather than a plotting artifact. Biophysically, iEEG reflects spatially summed local field potentials that low-pass filter underlying neural activity; these far-field signals aggregate excitatory and inhibitory processes and are not expected to show the sharp single-neuron tuning seen in spike recordings. As a result, broad peaks centered on the most strongly driven channels are expected. We have added text in the results section discussing these limitations, overall maps reduced from iEEG responses were similar in size and orientation compared to single unit maps, "albeit at coarser gradients likely due to aggregate recordings of excitatory and inhibitory activity and low-pass filtering due to potentials originating far from recording sites." We also added in the results section the comparison of spatial correlations (Fig. 2B,G) at the extremes of stimulus separation "electrode separations (CI 1 vs ≥5 electrodes, ERP: p=0.01, HG: p=0.04)" as analyzed by linear mixed effects models.

> *(1c) Mismatched frequency ranges*

We constricted the range of frequencies plotted in some panels (e.g., Fig. 2C from 1.4-32 kHz to 1.4-16 kHz) to emphasize the compressed range of tonotopic gradients and patterns.

> *(1d) The slopes in Figures 2B and 2G are non-significant*

We agree that non-significant group-level slopes indicate that CI-evoked tonotopy is weaker than tone-evoked tonotopy, and we now emphasize this point. At the same time, the data exhibit systematic structure: for both ERP and HG, mean spatial correlations decline monotonically with increasing CI channel separation (Fig. 2B,G). We also directly compared spatial correlations at the extremes of stimulus separations (1 vs. ≥5-channel separation) and found a significant difference. This is updated in the manuscript as: "At the extremes, the spatial correlations were always higher for small vs. large tone separations (NH 0.5 vs ≥3.5 octaves, ERP: $p<10^{-4}$, HG: $p<10^{-4}$ Student's one-tailed t-test) and electrode separations (CI 1 vs ≥5 electrodes, ERP: p=0.01, HG: p=0.04).". Together with the strong deviation from shuffled maps in the vector-strength analysis (Fig. 2E), we argue that analysis of spatial correlations indicates that CI-evoked maps are not random but reflect a coarse underlying gradient. In addition, as tone-evoked maps exhibit tonotopy, we asked if CI stimulation itself is at least spatially tuned in the periphery. Using ECAPs with a forward-masking paradigm (new Supplemental Fig. 1), we show that probe-evoked ECAPs are significantly more suppressed by adjacent than by distant maskers (N = 3), demonstrating functional spatial tuning of CI electrodes in the cochlea. We have also replotted these results in comparison with the same measurements from a human CI user (Author response image 1). This supports the interpretation that peripheral input is spatially specific and that the weaker cortical cochleotopy likely reflects the properties and resolution of iEEG and acute CI stimulation rather than a complete absence of spatial organization. Overall, the new comparative figures and analyses are intended to make transparent that (i) iEEG robustly captures tonotopy for acoustic tones, and (ii) CI-evoked CI-evoked responses exhibit coarser, but statistically non-random, cochleotopic organization.

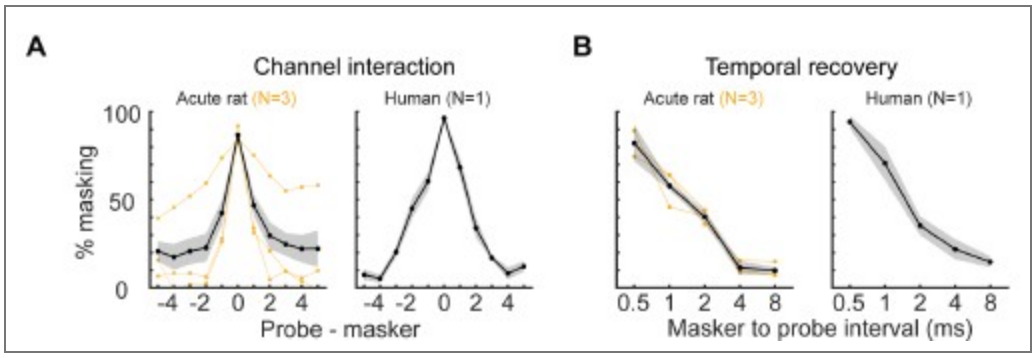

Author response image 1. Here, we compare data from the new Supplemental Figure 1C,D with human data (N=1) for spatial & temporal tuning in the periphery, as assessed by forward masking ECAP measurements. A) Spatial tuning functions were averaged across all probe electrodes and 3 animals (left) and 1 human subject (right) (black, mean; gray: s.e.m..; orange, average of individual subjects). B) Temporal tuning functions were averaged across all probe electrodes and 3 animals (left) and 1 human subject (right) (black, mean; gray, s.e.m.; orange, average of individual subjects). Note: human subject is the first-author, a long-term cochlear implant user (>10 years) with significant open set speech perception.

> *(2) The statistical approach is inappropriate where pairing is incomplete: a Student's paired two-tailed t-test is used despite not all data being paired; a linear mixed-effects model would be more suitable, whereas an unpaired test risks reduced power.*

We agree with this suggestion. As the reviewer notes (also raised by Reviewer 3), our original analyses did not fully exploit the partially paired structure of the data. In the initial submission we used paired t-tests when animals contributed both normal-hearing (NH) and CI measurements, which meant that animals with only NH or only CI data were excluded from those tests.

To address this, we have re-analyzed all NH vs. CI comparisons using linear mixed-effects models that incorporate both paired and unpaired observations within a single framework. This approach allows us to (i) include all available animals, (ii) appropriately account for within-animal dependence when both conditions are present, and (iii) align the statistical tests with the data shown in the figures. In nearly all cases, the mixed-effects models confirm our original conclusions. Two comparisons that were previously non-significant are now significant in the positive direction: Fig. 2E ($p = 0.048$) and Fig. 6F ($p = 0.027$, linear mixed-effects models). We have updated the manuscript to report these values and to clarify the use of mixed-effects modeling in the methods under the section titled, “Linear mixed effects modeling.”

> *(3a) Given the surgical complexity, objective verification of implantation and deafening is needed (e.g., eABRs for implant function and post-deafening ABR thresholds)”*

We agree that objective verification of both implant placement and deafening is critical, particularly given the surgical complexity of multichannel CI implantation in rats. Note that we previously extensively documented deafness in our cochlear implant rats with eABRs, histology of hair cell counts, and behavior (turning the implant off and seeing performance drop to chance). As we argued in Glennon et al. Nature 2023, the primary outcome measure and definition of deafness is behavioral, as anatomical and physiological markers are correlates of functional deafness but ultimately deafness must be defined in terms of behavioral performance. This is described in more detail below.

We agree that objective verification of both implant placement and deafening is critical, particularly given the surgical complexity of multichannel CI implantation in rats. Note that we previously extensively documented deafness in our cochlear implant rats with eABRs, histology of hair cell counts, and behavior (turning the implant off and seeing performance

drop to chance). As we argued in Glennon et al. Nature 2023, the primary outcome measure and definition of deafness is behavioral, as anatomical and physiological markers are correlates of functional deafness but ultimately deafness must be defined in terms of behavioral performance. This is described in more detail below.

Implant placement: Our primary concern during surgery is to ensure that the CI array is correctly positioned along the cochlear spiral toward the apex. As shown in Author response image 2, once the bulla is opened and the cochleostomy is made at the junction of the temporal bone and the stapedial artery, the orientation of the cochlear spiral is clearly visible under the surgical microscope. We advance the 8-channel array only in the apical direction, and we require that all 8 electrodes pass through the cochleostomy. A complete insertion of all 8 electrodes cannot be achieved with a basal-ward trajectory, so full insertion provides a strong anatomical confirmation that the array is directed apically. The white band on the array, visible just basal to the cochleostomy (Author response image 2), serves as a consistent visual marker of complete insertion. We have added text and this figure to the Methods to clarify these criteria, “We required that all eight electrodes pass through the cochleostomy, confirming that the array was inserted in the direction of the apex.”

Verification of deafening: We also share the reviewer’s concern about confirming profound hearing loss, particularly because some CI animals were presented acoustic tones to drive individual channels. We used the same mechanical-only deafening procedure described and validated in our previous work (King et al., 2016; Glennon et al., 2023), which was chosen to minimize systemic side-effects and maximize post-surgical survival, validated in three ways:

- Histology: In N=4 deafened animals, inner hair cell loss was ~50% and outer hair cell loss was near complete at almost 100% in all animals.

- Physiology: For N=14 rats, acoustic ABRs were substantial before deafening but statistically similar to baseline noise after deafening.

- Behavior: For N=16 deafened rats, behavioral performance with implant on was d': 1.7±0.1, but when implant was turned off in a subset of sessions, performance dropped to chance (d': −0.05±0.1, $P < 0.0001$).

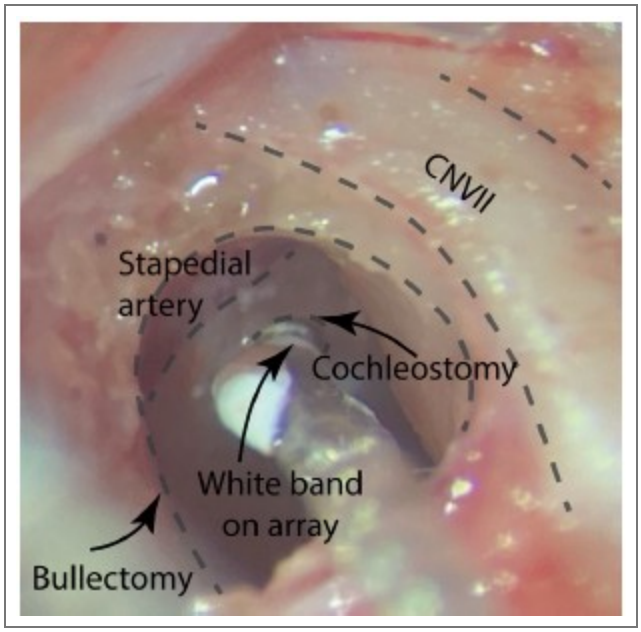

Author response image 2. Visual confirmation of a successful electrode insertion. The direction of an 8-channel array being implanted toward the apex is clear under microscope. Full insertion of all 8 channels is

further confirmed by the white band's (located after basal electrode) proximity to the cochleostomy.

This combination of histological, physiological, and behavioral evidence indicates that the mechanical-only deafening protocol produces profound hearing loss, with no functionally relevant residual hearing at intensities equal to or greater than those used in our study (70 dB SPL). Given this prior validation under identical surgical and experimental conditions, we are confident that our CI animals were effectively deafened and that the iEEG responses we report are driven by the implant rather than by residual acoustic hearing. We now clarify this in the Methods and explicitly cite our validation: "(mechanical only, as described and validated in Glennon et al. 2023).

> *(3b) One CI animal did not learn the task (Fig. 1C), potentially reflecting implantation efficacy.*

Good point, thanks. For both humans and rats, cochlear implant performance can be highly variable, reflecting a number of factors in terms of device performance, training efficacy and motivation, or other technical or biological sources of heterogeneity. We note however that not all animals included in this study were behaviorally trained, and wanted to show the full range of variable performance for the subset of animals that were trained (N=4 typical hearing and N=3 cochlear implant rats, one of the 4 trained animals lost the implant before it could be re-trained on the cochlear implant version of the task). We now highlight this range of performance variability in the results section and explain why N=4 normal-hearing and N=3 cochlear implant rats.

> *(4) The behavioural paradigm and cohort accounting are unclear: Figure 1C shows four NH-trained rats, yet subsequent analyses include only two NH-trained animals, which is confusing.*

We have now clarified the relation between the behavioral cohort and the iEEG cohort in the revised manuscript. The key point is that the animals in Figure 1C are defined by their behavioral training history (NH vs CI training), whereas inclusion in the iEEG analyses is defined by the specific stimuli collected during acute recordings, and these two categorizations are not always the same. In total, four rats underwent both iEEG recordings and behavioral training. Of these four, three were subsequently deafened, implanted with chronic CIs, and trained on the CI-driven task (Fig. 1C). With respect to the acute iEEG experiments, we obtained tone-only iEEG in 1 animal, CI-only iEEG in 2 animals, and both tone- and CI-evoked iEEG in 1 animal.

Thus, the "NH-trained" label in Figure 1C refers to behavioral training status, not to the stimulus conditions used during iEEG recordings. All iEEG measurements were acute and performed immediately after surgery (for CI animals) or in the normal-hearing condition, before any CI behavioral training. Consequently, the behavioral cohort in Figure 1C is larger than the subset of animals that contributed to specific iEEG contrasts in later figures, which explains why some panels include only two NH animals.

To clarify this, we have added a new Supplementary Figure 2 that provides a timeline for each animal, indicating when behavioral training occurred, when deafening and implantation occurred, and which stimulus conditions (tones vs CI) were used for each iEEG recording. We kept this figure in the Supplementary section because the focus of the manuscript is on evoked iEEG measurements rather than behavior, but the revised text now explicitly refers to this schematic when describing the cohorts "The combinations of animals that underwent behavioral training and acute iEEG measurements are shown in Supplemental Fig. 2."

> *(5) Methods lack essential details: specify acoustic stimulus types and intensities, CI stimulation parameters (e.g., current/charge per phase, phase width, rate, loudness*

> *setting), and the recording state (awake vs. anaesthetised), which is only implied in the discussion.*

We agree that these details are essential, and Reviewer 3 raised similar concerns about methodological clarity. We have now expanded the Methods to specify the acoustic stimuli, CI stimulation parameters, and recording state.

Acoustic stimuli: We now describe the acoustic stimulus set in the Methods, which references Insanally et al. (2016). Briefly, tones were pure sinusoids spanning frequencies from 1.4 to 32 kHz (half octave spaced), presented at 70 dB SPL with a duration of 50 ms with 2ms cosine-squared ramps and at a pseudorandom sequence of 1.25 Hz. These parameters are now updated in the methods under "Stimulus presentation for cortical sensory mapping in normal hearing rats."

CI stimulation parameters: CI stimulation used standard clinical-style monopolar mappings. We now specify in the Methods that pulses were biphasic, charge-balanced, with 8 μs interphase gaps and 25 μs /phase (total pulse width = 58 μs); stimulation rate was 900 pulses per second (pps); and current amplitude (and thus charge per phase) was set individually for each electrode based on its ECAP threshold. All stimulation levels were within normal and safe limits: charge densities remained below the Shannon limit and within the electrochemical "water window."

Loudness setting: In this study, CI stimuli were presented primarily at a single level—each electrode was stimulated at its ECAP threshold level for the tone-to-CI mapping experiments. We have added these details in the methods under the "Stimulus presentation for cortical sensory mapping in cochlear implanted rats" subsection.

Recording state: All iEEG recordings reported in the manuscript were acute and performed under anesthesia. This is now stated explicitly at the start of the Methods section.

> *(6) Plasticity and training effects warrant further consideration: although the manuscript reports no difference between naïve and trained rats, Figure 3 suggests greater across-trial variability for CI than NH that is not evident in the trained subset; examining relationships among behavioural performance, decoder performance, across-trial variability, and training duration would strengthen interpretation.*

We agree that plasticity and training effects are central questions for cochlear implant research and that iEEG is well suited to study how cortical representations evolve with CI use. However, the current dataset was collected mainly to compare cortical encoding of acoustic versus CI stimulation under matched, acute conditions (not necessarily after behavioral training with the implant, and we note that most studies of physiological responses to cochlear implant function in non-human species also do not incorporate aspects of training). All CI-evoked iEEG recordings were obtained immediately after implantation, before any CI-based behavioral training. As a result, any training effects reflected in the iEEG data can only arise from prior normal-hearing training, not from experience with CI stimuli themselves. Only a small subset of animals (N = 3 of 10) underwent behavioral training with cochlear implants, and their training histories (duration, performance levels, CI hardware status) are not uniform. This yields insufficient statistical power to meaningfully examine correlations among behavioral performance, decoder performance, across-trial variability, and training duration. While we note the reviewer's observation that across-trial variability appears qualitatively different in the small, trained subset, we do not believe the current data justify strong conclusions about training-related plasticity.

> *(7) Differentiating the CI rats stimulated directly or through the microphone of the speech processor -at least in the figures - would be useful to allow the reader to assess whether both stimulation strategies give rise to similar results.*

We agree that it is important to distinguish between rats stimulated directly via CI hardware and those stimulated acoustically through a speech processor. We now show in new Supplementary Figure 2, which animals received direct electrical stimulation and which were driven acoustically through the processor microphone. We also now plot tonotopic and cochleotopic maps for all CI animals in Supplementary Figure 3, with the stimulation mode indicated for each animal. As discussed in our response to comment #2 of Reviewer 3, we also provide validation that acoustic tones can be used to selectively drive individual electrodes via the speech processor. However, the sample sizes for the two stimulation strategies are small (N = 4 rats with direct CI stimulation, N = 3 rats with acoustic CI stimulation). For this reason, we have chosen not to draw strong statistical conclusions about differences between direct vs acoustic CI stimulation in the present manuscript.

> *(8) Typographical error at the end of the introduction ("To this end we have designed and manufactured..."), and in the first paragraph of the Discussion ("...that both that...").”*

Thanks, we have updated the manuscript accordingly.

> *(9) Inconsistent terminology: use a single form (e.g., "normal-hearing") throughout.*

Good suggestion, thanks. We have updated all main manuscript to only use normal-hearing. We found and changed two instances in which we used the acronym NH in lieu of normal-hearing, once early in the results section and once in the legend for Figure 3.

> *(10) In Figure 3D (temporal), there appears to be an extra data point for the NH-trained group.*

Thank you for flagging this mis-labeling, which Reviewer 3 also pointed out. We have switched the appropriate data point in Figure 3D from ‘trained’ to ‘naïve’.

> *(11) In Figure 4D, the yellow line is not defined; based on Figure 6D, it likely represents shuffled/chance performance and should be labeled accordingly (including beneath the chance line on the plots).*

We have updated Figure 6 to indicate that the yellow line does indeed reflect shuffled/chance.

> *(12) Figure 8 would benefit from a control demonstrating that poor cross-modal decoding reflects train-test distribution differences rather than weak decoders (e.g., train on a subsample of NH and test on held-out NH), and from reporting decoding on raw ERP/HG features in addition to TCA-derived data.*

Good suggestion, thanks; we have now added this control. We agree that a positive control is necessary to show that poor tone→CI decoding reflects differences of underlying representations rather than a failure of the decoder or modeling approach. (Reviewer 2 raised the same point.)

To validate our cross-modal analysis pipeline, we re-implemented the full procedure used in Figure 8, but instead of training on tone-evoked responses and testing on CI-evoked responses, we trained and tested on independent sets of tone-evoked trials from the same animals (tone→tone). For each tone in each animal, we withheld 10 trials as a test set. Using the remaining trials, we fit the original TCA model to obtain spatial and temporal factors (Fig. 8A). We then fixed these factors and re-optimized only the trial factors on the withheld tone-evoked trials (Fig. 8B). The LDA decoder was trained on the trial factors from the original TCA fit and tested on the re-optimized trial factors from the withheld trials, using the same classification pipeline as in the main analysis.

As shown in the top panels of Figure 8C,D, this positive control yielded robust tone→tone generalization: predicted tone frequencies closely matched the actual tones, decoder

performance was significantly above chance, and prediction errors were tightly clustered around the true stimulus, indicating that the decoder was tuned to tone frequency. In contrast, when we trained on tone-evoked responses and tested on CI-evoked responses, information transfer was markedly reduced (Fig. 8E-G).

These results demonstrate that the TCA+decoder pipeline can reliably transfer information across independent tone-evoked datasets, confirming that the method captures shared structure when it exists. The poor cross-modal transfer between tone- and CI-evoked activity therefore is unlikely to be due to a weak decoder or to a failure of the modeling pipeline, but instead reflects a genuine mismatch between CI and sound representations in auditory cortex. We have updated Figure 8 and the Results section to describe this positive control analysis and clarify the interpretation.

> *(13) Perception and interpretation of signals are mentioned several times in the introduction, although perception is not explored in the manuscript (only neuronal processing). This might be confusing.*

We appreciate the need to distinguish between neuronal encoding and perception. We also feel we have been careful not to invoke relationships to perception when presenting analyses on iEEG measurements, but we did identify an opportunity to further clarify this distinction between neuronal processing and perception by adding text in the intro, as follows “for the auditory system to interpret patterns of evoked neural activity and inform downstream auditory areas.”

> *(14) Figure 1C. Why is the performance of CI rats so much lower than what was previously published (Glennon et al., 2023)? Did the training duration change?*

The three animals that were behaviorally trained on the normal-hearing (pre-deafening) and cochlear implant task (post-deafening) are within the distribution of the full set of animals from Glennon et al. (2023). However, we note that for Glennon et al. (2023), as one of our behavioral criterion was days to d’ > 1, animals were trained daily until reaching that level and not included in the initial data set if they did not reach that level. However, as we were including animals in this study of iEEG responses that were not trained at all, we felt it appropriate to include this third animal as well, that was trained just for 3 days before recordings were made. The two other animals were trained for 9 and 13 days. We have now included this information in the methods.

(15) The p-values = 0.5 should be given with an additional digit.

We previously rounded to the nearest single decimal digit, for all p-values greater than 0.10. We have updated the figures and manuscript text to ensure precision at least to the second digit.

> ***Reviewer #2 (Recommendations for the authors):***

We thank the Reviewer for their thoughtful comments on our study.

> *(1) Less noisy recording methods based on spike detection would provide stronger claims.*

We agree that spike recordings, particularly isolated single-unit activity, are powerful for testing hypotheses about sensory encoding in auditory cortex, and we plan to incorporate such approaches in future work. However, our decision to use iEEG arrays in the present study was deliberate and central to the scientific and translational goals of the project.

First, iEEG and related population-level approaches such as scalp EEG (e.g., Lalor and Foxe, 2010; O’Sullivan et al., 2015) and fNIRS (e.g., Bortfeld et al., 2009; Peelle, 2017) are widely used in humans and have been highly successful in decoding sound- and speech-evoked responses,

revealing fundamental principles of how sound and speech are encoded in the human brain. Because speech is uniquely human and cochlear implants are primarily designed to restore speech perception, aligning our recordings with clinically relevant, human-used modalities enhances the translational relevance of our work.

Second, iEEG arrays provide distinct advantages over modern multi- and single-unit electrophysiology. Even with high-density probes, the spatial sampling of neuronal activity does not match the coverage of the 60-channel iEEG arrays used here, which span large extents of auditory cortex. One might instead consider optical methods such as calcium imaging to interrogate topographical encoding at single-neuron and mesoscale resolutions, as has been done in normal-hearing mice (Romero and Hight et al., 2019). However, calcium signals are intrinsically slow, limiting access to the temporal precision that is critical for CI encoding, and these tools are unlikely to be available in humans in the foreseeable future, substantially reducing their translational value.

Using iEEG arrays, we show that CI-evoked responses are topographically organized, consistent with prior work (Klinke et al. 1999, Bierer and Middlebrooks 2002, Middlebrooks and Bierer 2002, including Adenis et al., 2024 now referenced in the manuscript). Our study extends these findings by exploiting simultaneous recordings across both spatial and temporal domains, which are essential for several key analyses (Figs. 3-8), including quantification of trial-by-trial variability, decoding of stimulus identity from single trials, and cross-modal comparisons between normal-hearing and CI-evoked iEEG responses.

Thus, we believe that the strength of this study is due to, rather than in spite of, its use of iEEG arrays. This approach uniquely allows us to test hypotheses about CI encoding across cortical topography and time using a modality that is directly translatable to human research and clinical practice. In response to the reviewer's concern, we have also (i) improved the statistical treatment of our data (by adopting linear mixed-effects models that incorporate both paired and unpaired observations), (ii) added additional positive controls (see response to comment #2), and (iii) collected new data that further validate our rodent CI model. Together, these additions strengthen the support for our conclusions while preserving the key advantages of the iEEG-based approach.

> *(2) A positive control is necessary to claim the mismatch between CI and sound representations.*

We agree. We now have added a positive control specifically designed to validate our cross-modal analysis pipeline in our revised manuscript. As also suggested by Reviewer 1, the goal was to test whether our method can successfully transfer information when the training and test datasets are matched in modality (tone→tone), thereby ensuring that the observed failure of cross-modal transfer (tone→CI) is not an artifact of the analysis.

To do this, we re-implemented the full pipeline used in Figure 8, but instead of training on tone-evoked responses and testing on CI-evoked responses, we trained and tested on independent sets of tone-evoked trials from the same animals. For each tone in each animal, we withheld 10 trials as a test set. Using the remaining trials, we fit the original TCA model to obtain spatial and temporal factors (Fig. 8A). We then fixed these factors and re-optimized only the trial factors on the withheld tone-evoked trials (Fig. 8B). The LDA decoder was trained on the trial factors from the original TCA fit and tested on the re-optimized trial factors from the withheld trials, using the same classification pipeline as elsewhere in the manuscript.

As shown in the top panels of Figure 8C,D, this positive control yielded robust tone→tone generalization: predicted tone frequencies closely matched the actual tones, decoder performance was significantly above chance, and prediction errors were tightly clustered around the true stimulus, indicating that the decoder was tuned to tone frequency. In

contrast, when we trained on tone-evoked responses and tested on CI-evoked responses, information transfer was markedly reduced and not different from shuffled controls (Fig. 8E-G).

These results demonstrate that the TCA+decoder pipeline can reliably transfer information across independent tone-evoked datasets, confirming that the method captures shared structure when it exists. The poor cross-modal transfer between tone- and CI-evoked activity therefore cannot be attributed to a failure of the modeling pipeline but instead reflects a mismatch between CI and sound representations in auditory cortex. We have updated Figure 8, the methods, and the results section to include this new important analysis.

> ***Reviewer #3 (Recommendations for the authors):***

We thank reviewer 3's appreciation for study design and the appropriateness of analyses taken. We also appreciate the recognition of noteworthiness, specifically that stimulus identity can be decoded on a single-trial basis and of the potential benefit of using central decoders in clinical settings.

> *(1a) Animal heterogeneity: It is difficult to keep track of the animals used in this study, and some received a different protocol of stimulation (sounds through the speech processor vs. direct stimulation) and were also trained in a behavioral task using different target stimuli (4kHz vs. 22.6kHz, also no mention of the CI electrode used as a target).*

We have now clarified the animal cohorts and stimulation protocols in our revised manuscript. We added a new Supplementary Figure 2 that schematizes, for each animal if it underwent behavioral training with pure tones in the normal-hearing condition, if tone-evoked iEEG measurements were collected, if CI-evoked iEEG measurements were collected (and whether stimulation was direct or via the speech processor), and if it subsequently received CI-based behavioral training. Regarding the behavioral targets, we now specify in the Methods that for normal-hearing training, the target stimulus was a 22.6-kHz pure tone. For CI-trained animals, the target was either CI channel 3 (n = 2 rats) or CI channel 4 (n = 1 rat). Details about stimuli targets during behavior have been added to the methods section under "Behavioral training for tone and implant channel detection."

> *(1b) There is no comparison of the CI maps from rats tested with the speech processor and directly stimulated. How different were they? Was the frequency allocation of each electrode the same for each animal? Since data might already have intrinsic variability because of the grid placement, the mechanical deafening, and the cochlear implantation in each animal, such heterogeneity in the 'background' and stimulation protocol might blur the authors' results.*

Our study focuses on cortical encoding of single-channel CI stimulation, so it is indeed important to ensure that the stimuli are effectively delivered by a single electrode, regardless of whether they are driven acoustically via the speech processor or by direct electrical stimulation.

Stimulation mode and frequency allocation: The project began with single-channel stimulation achieved by presenting pure tones to the speech processor (N=3 animals) and later transitioned to direct programmatic control of individual electrodes (N=4 animals) to simplify the experimental setup. In both cases, the goal was to activate only one CI channel at a time.

For the programming speech-processor animals, the validation protocol described in Glennon et al. (2023) is as follows:

- Set the number of active channels in the processor to 1 (the clinical default is 8) to avoid spectral spread across electrodes.

- Disabled all additional signal-processing strategies (e.g., Scan, ASC, ADRO, SNR-NR, WNR).

- Used customized frequency allocation tables that mapped narrow frequency bands to individual electrodes, as shown in Glennon et al., 2023, Extended Data Fig. 2.

To confirm that a given tone drove only the intended electrode, we recorded tone-evoked electrodograms—measurements of the output at each electrode—and verified that only the targeted channel was active (Glennon et al., 2023, Extended Data Fig. 2). Thus, although the initial CI drive was acoustic, the effective stimulation at the array was restricted to a single electrode with a well-defined frequency allocation.

For the direct-stimulation animals, we used the same underlying frequency allocations to choose which electrode to stimulate, but the pulses were delivered programmatically rather than via the speech processor. In both modes, the center frequency associated with each electrode was therefore defined consistently across animals, and stimulation was confined to one channel at a time.

Comparison of maps across stimulation modes: We now explicitly indicate the stimulation mode (speech-processor vs direct) for each CI animal in Supplementary Figure 2 and plot the maps for all animals in Supplementary Figure 3. Qualitatively, the spatial organization of CI-evoked maps is similar across the two stimulation strategies; we do not observe systematic differences in map structure that would suggest large biases introduced by the stimulation mode. However, the sample sizes for each group are small (N = 3 speech-processor, N = 4 direct). For this reason, we have not performed formal between-mode statistics and instead treat stimulation mode as a source of minor heterogeneity, alongside inevitable variability from grid placement, mechanical deafening, and cochlear insertion. Given the electrodogram validation (Glennon et al., 2023, Extended Data Fig. 2) and consistent frequency allocation tables, we are confident that both approaches produce single-channel activation with comparable effective frequency assignments.

> *(1c) The number of animals used is also confusing. The authors report 7 NH and 7 CI animals (14 total), 4 NH and 3 CI were trained before being implanted (so 3 naïve NH and 4 naïve CI remain). Figure 1C reports that only 3 trained NH performed with the CI (let us call them 3 NH->CI). But then Figure 1E reports only 1 trained NH->CI and only 1 trained NH and 3 naïve NH that got implanted later. On the other hand, Figure 1E reports only 1 true naïve CI animal, the 3 others being naïve NH that got implanted. For the sake of clarity, I would encourage the authors to provide a timeline of the procedures/stimulation protocols coupled with a schematic distribution of the animals.*

To address this, we have added a new Supplementary Figure 2 that provides, for each individual animal a chronological timeline (NH recordings, deafening, implantation, CI recordings); if it was behaviorally trained in the NH condition, the CI condition, or both; if CI stimulation was delivered via the speech processor or by direct electrical stimulation; and which stimulus conditions (tone-evoked iEEG, CI-evoked iEEG) were collected. This schematic makes it clear how the reported totals arise (7 NH and 7 CI for iEEG; 4 NH-trained and 3 CI-trained behaviorally) and shows which specific animals contribute to each panel in Figure 1 and to the later iEEG analyses. We now reference Supplementary Figure 2 in the Results when introducing the cohorts to guide readers through animal accounting.

> *(2a) Methods and statistics: Deafening is only mechanical, with no direct or postmortem proof that deafening was complete. The authors cite previous studies, but that would have been a good control to have since mechanical deafening isn't as accepted as the*

> *chemical deafening, like Neomycin, especially when some of your animals were stimulated with pure tones through the speech processor."*

We agree that rigorous verification of deafening is essential, particularly when some CI animals are driven acoustically through the speech processor. Ototoxic approaches (e.g., systemic or local neomycin) are one established method, but their effectiveness can be sensitive to dose and delivery, and they introduce systemic side-effects that can complicate long-term survival and recovery.

Our laboratory has used the mechanical deafening procedure since it was first described in King et al. (2016) and more recently in Glennon et al. (2023). In King et al., mechanical and ototoxic methods were combined, and we found that ototoxic methods provided no more additional robustness in deafening compared to mechanical lesion. Instead, the additional time required for ototoxic drug application reduced survival times in what was already a very complex and long surgical procedure for bilateral deafening and unilateral cochlear implantation.

In Glennon et al. (2023) we intentionally employed mechanical-only deafening to minimize side-effects while still achieving profound hearing loss in implanted animals. Glennon et al. (2023) provides an extensive validation of this mechanical-only protocol under the same surgical and experimental conditions as the present study. As we mentioned in our response to comment #3a of Referee 1, we assessed deafness through three measures:

Histology: In N=4 deafened animals, inner hair cell loss was ~50% and outer hair cell loss was near complete at almost 100% in all animals.

Physiology: For N=14 rats, acoustic ABRs were substantial before deafening but statistically similar to baseline noise after deafening.

Behavior: For N=16 deafened rats, behavioral performance with implant on was d': 1.7±0.1, but when implant was turned off in a subset of sessions, performance dropped to chance (d': −0.05±0.1, $P < 0.0001$).

This convergent anatomical, physiological, and behavioral evidence demonstrates that the mechanical procedure produces profound deafness, with no functionally relevant residual hearing at levels ≥90 dB SPL. Also as we mentioned in response to comment #3a of Referee 1, we believe that the behavioral criterion is most essential and also least common in the literature. Because the tones used to drive the speech processor in the current study were presented at 70 dB SPL, we have no reason to believe that residual acoustic hearing contributed to any of the CI-evoked responses we report.

We now cite these validation data explicitly in the methods under the section "Bilateral sensorineural hearing loss" as follows "(mechanical only, as described and validated in Glennon et al. 2023)" to make clear why we consider the mechanical-only approach sufficient for ensuring deafness in the present experiments.

> *(2b) What motivated the selection of 15 Principal Components for the PCA? That might need to be justified, maybe by scree plot or variance plot (Eigen Values or CEV), as if too many PCs are selected, you are at risk of losing information. Side comment for TCA: why is it important that the number of latent factors exceeds the number of tones or stimuli? Is there a way to justify this statement?*

We thank the reviewer for raising this point. Our choice of 15 components/latent factors was motivated by both theoretical and empirical considerations, which are now made explicit in the manuscript.

For the PCA analyses, we selected 15 principal components for two reasons. First, because our decoder must discriminate between 10 tone conditions, we reasoned that providing at least as many dimensions as stimuli would be beneficial, while also allowing for the possibility that some components may carry little or no stimulus-selective information. We therefore chose a modest number of components that exceeded the number of tones (10) but avoided unnecessarily high dimensionality. Second, we empirically examined the variance explained as a function of the number of components. As shown in the new scree plots (Supplemental Fig. 4A), the cumulative variance explained enters a near-linear, low-slope regime beyond ~15 PCs, indicating diminishing returns for including additional components. Thus, 15 PCs capture a substantial fraction of the stimulus-related variance while minimizing the risk of overfitting and retaining a consistent dimensionality across animals.

For the TCA analyses, we used 15 latent factors to match the dimensionality used in PCA and to ensure that the latent space was sufficiently flexible to represent the 10 tone conditions without being under-parameterized. In practice, increasing the number of TCA components reduces reconstruction error (Williams et al., 2018), but with diminishing improvement beyond a certain point. We therefore systematically evaluated model error as a function of the number of latent factors and found that error decreased rapidly up to ~15 components and then plateaued (Supplemental Fig. 4B). This pattern parallels the PCA scree plots and supports 15 as a reasonable trade-off between model flexibility and parsimony.

We have updated the Results clarify these choices, as follows “The number of components (15) was chosen based on PCA scree plots (Supplemental Fig. 4A), which showed that explained variance entered a near-linear, low-slope regime beyond this point demonstrating a similar plateau in reconstruction error (Supplemental Fig. 4B).”

> *(2c) Legend of Figure 2E, J states that a Student's paired t-test was used, meaning that only the 'linked' points of the graph were used (thus, comparing only animals that got tested NH then implanted). This is usually the same across the manuscript. Why not include all the points with an unpaired t-test? Otherwise, why are all the points plotted if they serve no purpose? This choice should be justified.*

We agree with this concern, which was also raised by Reviewer 1. We have revised our statistical approach accordingly in our revised manuscript. In the original submission, we used paired t-tests when animals contributed both normal-hearing (NH) and CI data, which meant that animals with only NH or only CI measurements were excluded from those comparisons even though they were shown in the plots.

To address this, we have re-analyzed all normal-hearing vs. CI comparisons using linear mixed-effects models that include both paired and unpaired data within a single framework. This approach ensures that every plotted data point contributes to the statistical tests, properly accounts for within-animal dependence when both conditions are present, and avoids the loss of power that would arise from either paired-only or purely unpaired tests.

The mixed-effects results are consistent with our original interpretations, with two comparisons becoming significant in the updated analysis: Fig. 2E ($p = 0.048$) and Fig. 6F ($p = 0.027$). We have updated the Results and figure legends to describe the use of mixed-effects models and to report these revised p-values. Together with the new tonotopy and cochleotopy analyses described above, these changes strengthen the statistical support for our conclusions without altering the overall interpretation of the data.

> *(2d) Side comment: There are inconsistencies on the bar plots of Figure 6C (Missing a purple point) and Figure 3D (Temporal has 3 purple points).*

Thank you for flagging this mis-labeling (which Reviewer 1 also noticed). We have correctly updated the appropriate data point from trained to naive for Fig. 3D and from naive to trained for Fig. 6C.

> *(3a) Pure tones and CI-evoked responses maps: It is the reviewer's understanding that Figure 2 is an averaged representation for all animals. Why is the tonotopic shift so dim for ERPs? The averaged maps aren't very convincing. How were the gradients on an animal-to-animal basis since Figure 2D is only an example animal? Also, everything has been evaluated at 70dB, where selectivity might not be best. It would have been easier to follow the tonotopic gradient at the CFs where contrasts are higher.*

We agree that the strength and interpretation of tonotopy/cochleotopy in our iEEG data needed to be presented more clearly. Reviewer 1 raised closely related concerns, and we have substantially expanded the analyses and explanations in response. Here we highlight the points that address your specific questions.

Single-animal vs. averaged maps: We included both exemplar maps and population summaries in Figure 2. The panels analogous to Figure 2D show single-animal best-frequency (BF) or best-channel maps; these were chosen because they exhibit clear, interpretable gradients. In the exemplar shown, there is a local high-frequency (HF) region along the medial edge of the array that transitions to lower frequencies toward the rostral edge. For CI-evoked best-channel maps in the same animal, we observe a parallel pattern in which basal electrodes (e.g., electrode 8, representing higher frequencies) occupy the HF region and apical electrodes (e.g., electrode 1, lower frequencies) occupy the LF region.

Averaged ERP maps, by contrast, necessarily blur some of this structure because iEEG is a summed field potential and animal-to-animal differences in array placement, cochlear insertion depth, and anatomy introduce variability. We have softened the language in the text to reflect that ERP-based tonotopy is coarse and weaker at the population level, while emphasizing that robust gradients are evident in single animals and in HG-based measures.

Quantitative assessment across animals: To move beyond visual impressions, we added quantitative analyses that mirror those used in Romero and Hight et al. (2020) for calcium imaging data (Romero and Hight et al. 2020 and Fig. 2). For each map we computed local tonotopic gradient vectors at every pixel and summarized their magnitude/direction on a unit circle, then compared the mean vector strength to shuffled maps. Applied to our BF and best-channel maps, this analysis shows that both are significantly more ordered than shuffled controls ($p < 10^{-10}$), indicating that the maps are tonotopic/cochleotopic rather than random, despite the apparent dimness of the gradients in some averaged ERP plots. These new results are described in the revised manuscript and shown in Romero and Hight et al. 2020 and Fig. 2.

Effect of intensity (70 dB SPL) and “dim” gradients: We agree that stimulus level influences the apparent sharpness of tonotopy. Higher intensities tend to broaden tuning and compress the dynamic range of BF maps. As we now discuss in more detail (adapted from our response to Reviewer 1), tones were presented at 70 dB SPL, so we expect maps to emphasize mid-frequency regions (around 8 kHz) and to show somewhat broader tuning than maps derived at threshold. For CI stimulation, we used ECAP thresholds to set intensity, which is effective in our preparation because animals can robustly discriminate individual electrodes and these electrodes evoke clear cortical activity (King et al., 2015; Glennon et al., 2023).

In summary, we clarified which panels in Figure 2 show single-animal exemplars vs population summaries, added quantitative analyses demonstrating spatial correlations are greater for adjacent stimuli compared to far-apart stimuli, and expanded the discussion of how recording modality and stimulus level influence the visibility of tonotopic gradients.

These changes are intended to make the evidence for tonotopy/cochleotopy in our iEEG data (and its limitations) more transparent.

(3b) Since new experiments might not be available, it is the reviewer's suggestion to add a supplementary figure showing a couple of animal examples following the format of Figures 2A and 2C that have more contrasted gradients to strengthen the group data. In the case of the CI-evoked responses map, this might also provide another argument to dismiss the potential monopolar smearing.

Good suggestion, thanks. We now include a new Supplementary Figure 3 that shows additional single-animal examples for both tone-evoked and CI-evoked maps, following the same format as Figure 2C.

Regarding monopolar stimulation, we agree that monopolar configurations are expected to be less spatially specific than bipolar or multipolar modes because current returns to an extracochlear reference electrode, potentially broadening the spread of excitation. We nevertheless chose monopolar stimulation because it is the predominant clinical configuration in human CI users and therefore most relevant for translational purposes. We acquired ECAP measurements of peripheral (spatial and temporal) tuning via a forward masking paradigm and demonstrate that monopolar is effectively tuned (Supplemental Fig. 2). Together with additional single-animal maps in Supplementary Figure 3, together with our vector-strength analysis (Romero and Hight et al. 2020 and Fig. 2), demonstrate that even under acute monopolar stimulation we observe structured cochleotopic organization in cortex, rather than the fully smeared patterns one might expect if monopolar spread completely dominated.

We also note that all CI-evoked iEEG measurements were made acutely, immediately after implantation and before any CI-based behavioral experience. It is possible that with longer-term use and plasticity, cortical cochleotopy could become sharper than what we observe here under acute conditions. In this sense, our data provide a conservative baseline showing that even at the earliest stages of CI use, monopolar stimulation already engages tonotopically selective regions of auditory cortex. A longitudinal comparison of acute versus chronic maps would be an interesting direction for future work but is beyond the scope of the current study.

> *(3c) Side comments: The legends of Figures 2D and 2I should mention that this is an animal example and not group data, as the rest of the figures are group data.*

Thank you for this suggestion to improve figure clarity. We have updated all of our figures, where appropriate, to indicate whether data are single or groups of animals.

> *(3d) In general, some of the legends should be revised because they are sometimes too "strong". As an example, Figure 3B, D legend states: "Variability of iEEG measurements across trials (root mean square, rms) was consistently higher for cochlear implant-evoked compared to tone-evoked activity", despite three of the statistical tests being non-significant. The manuscript is correct, on the other hand.*

Good point. We revised the legend for Figure 3 to be consistent with the figure and the manuscript.

> *(3e) The example spatial map given in Figure 3A for CI might not be the best choice since it is showing a pretty reliable trial-by-trial response, while your group data proves the opposite.*

We understand the reviewer's concern and agree that the exemplar CI map in Figure 3A appears relatively reliable on a trial-by-trial basis. This example was chosen deliberately from an animal in which we had both NH- and CI-evoked iEEG recordings, so that the reader

could visually compare the two conditions within the same preparation. In this animal, as in the group data, the differences between NH and CI trial-by-trial responses are subtle rather than dramatic.

Our group-level analysis shows that the RMS error across trials is consistently higher for CI-evoked than for NH-evoked responses, but the absolute differences are small (< 0.1) and relatively uniform across animals. The spatial maps plotted in Figure 3A are representative of this pattern: both conditions show reasonably robust evoked responses, with CI responses nonetheless showing slightly greater variability. To avoid implying a stronger qualitative difference than is supported by the data, we have revised the text to emphasize that (i) CI-evoked responses remain clearly detectable on single trials, and (ii) the key effect is a small but consistent increase in variability across animals, as captured by the RMS error metrics, "We noted that the differences were qualitatively subtle (Fig. 3A, right panel), they were consistent across animals (Fig. 3B)."

> *(4a) Decoders for CI stimulation Regarding CI stimulation, Pearson's correlations were truncated at a spacing of 5 electrodes. Likewise, none of the LDA classifiers show prediction for channels past CI-6. Again, that choice should be justified, or the missing channels should be presented.*

We truncated the correlation between electrodes at 5 because beyond that, the estimated means are significantly noisy. These estimated means are noisy because the number of data are significantly reduced, also significantly increasing the standard error. For example, for the maximum stimulus spacing, the number of pairwise correlations is at maximum the number of animals tested (i.e., N=7). We believe it's important to be transparent, so we have included the non-truncated version of the figure here in this public review (Author response image 3). We leave the figures in the manuscript untouched but have updated the Figure 2 legend justify this selection of data.

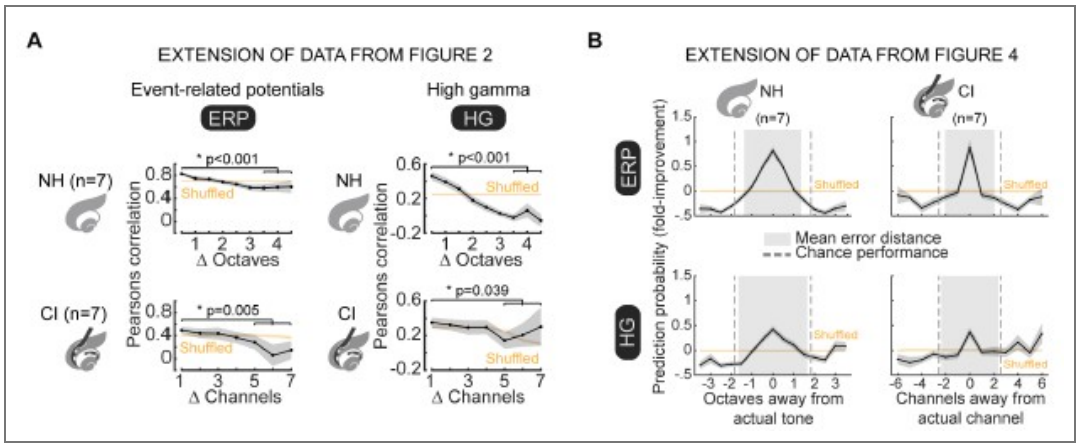

Author response image 3. Expanded figures for spatial correlations and LDA performance. A) The same data from manuscript Figure 2 are re-plotted but with expanded x-axes to include up to 4.5 octaves and 7 channels. Due to the smaller numbers of data at these points, the estimates for the mean spatial correlations are noisier. In all cases, the mean correlations are significantly higher for the first data point compared to the last 3 (NH, ERP p<0.001; NH, HG p<0.001; CI, ERP p=0.005; and CI, HG p=0.39, linear mixed effects models). B) The same data from manuscript figure 4 are re-plotted but with expanded x-axes to include up to ±3.5 octaves and ±6 channels.

> *(4b) Finally, retrained PCA-LDA on spatial-only and temporal-only for CI are absent in Figure 3D. Since the authors were pretty consistent in showing both NH and CI alongside in the rest of the paper, it would be coherent to add the CI counterpart to Figure 3D, or maybe with a supplementary figure.*

We agree that consistency can be improved by including classifiers for CI-evoked measurements, though presumably for Fig. 6C and not Fig. 3D. Figure 6 has been updated accordingly.

https://doi.org/10.7554/eLife.108550.2.sa0